



# Alkaline lake settings for concentrated prebiotic cyanide and the origin of life

J.D. Toner\*, D.C. Catling

*University of Washington, Box 351310, Dept. Earth & Space Sciences, Seattle, WA 98195, USA*

Received 4 April 2019; accepted in revised form 18 June 2019; Available online 25 June 2019

## Abstract

Cyanide plays a critical role in origin of life hypotheses that have received strong experimental support from cyanide-driven synthesis of amino acids, nucleotides, and lipid precursors. However, relatively high cyanide concentrations are needed. Such cyanide could have been supplied by reaction networks in which hydrogen cyanide in early Earth's atmosphere reacted with iron to form ferrocyanide salts, followed by thermal decomposition of ferrocyanide salts to cyanide. Using an aqueous model supported by new experimental data, we show that sodium ferrocyanide salts precipitate in closed-basin, alkaline lakes over a wide range of plausible early Earth conditions. Such lakes were likely common on the early Earth because of chemical weathering of mafic or ultramafic rocks and evaporative concentration. Subsequent thermal decomposition of sedimentary sodium ferrocyanide yields sodium cyanide (NaCN), which dissolves in water to form NaCN-rich solutions. Thus, geochemical considerations newly identify a particular geological setting and NaCN feedstock nucleophile for prebiotic chemistry. © 2019 The Authors. Published by Elsevier Ltd. This is an open access article under the CC BY license (<http://creativecommons.org/licenses/by/4.0/>).

**Keywords:** Prebiotic chemistry; early Earth; Origin of life; Cyanide; Alkaline lakes

## 1. INTRODUCTION

Cyanide is a key ingredient in organic synthesis experiments seeking to understand prebiotic chemistry because it is a strong nucleophile (i.e. a compound that donates electron pairs to build carbon-carbon chains and C-N groups) that forms polymers, nitriles, and cyanohydrins (Sanchez et al., 1967; Miller and Orgel, 1974; Ferris and Hagan, 1984). Recent origin of life research shows that many prebiotic organic compounds can be produced simultaneously from cyanide in reaction networks involving copper, sulfur, phosphorus, and UV light (Patel et al., 2015; Ritson et al., 2018). Cyanide needed for these reactions was likely present on the early Earth due to production of hydrogen cyanide (HCN) from photochemistry (including in expected CO<sub>2</sub>-rich atmospheres) (Zahnle, 1986; Tian et al., 2011),

high temperature reactions during asteroid impacts (Fegley et al., 1986; Ferus et al., 2017; Parkos et al., 2018; Shtyrlin et al., 2019), electrical discharges (Stribling and Miller, 1987; Cleaves et al., 2008; Ferus et al., 2017), and cometary inputs (Matthews and Minard, 2006). HCN gas in the atmosphere dissolves in rainwater and so would have been deposited onto the early Earth's surface.

A major problem for cyanide origin of life hypotheses is that relatively high cyanide concentrations are needed. At least ~10 mM HCN is required for polymerization (Sanchez et al., 1967) and published prebiotic schemes commonly use 1 M HCN (Patel et al., 2015), which is much higher than oceanic concentrations estimated from atmospheric deposition rates (Stribling and Miller, 1987; Miyakawa et al., 2002). Low oceanic cyanide is caused by dilution of HCN inputs, followed by slow decay with water to form formamide (Miyakawa et al., 2002) and reaction with formaldehyde to form glyconitrile (Schlesinger and Miller, 1973) (Supplementary Material, Appendix A).

\* Corresponding author.

E-mail address: [toner2@uw.edu](mailto:toner2@uw.edu) (J.D. Toner).

Hence, prebiotic cyanide chemistry requires an environmental mechanism for concentrating and protecting cyanides from decay.

Some studies have qualitatively hypothesized that cyanides could have concentrated in surface environments on the early Earth as aqueous and crystalline ferrocyanides (Keefe and Miller, 1996; Patel et al., 2015). Aqueous ferrocyanide forms via the following reaction:  $\text{Fe}^{2+} + 6\text{CN}^- \rightleftharpoons \text{Fe}(\text{CN})_6^{4-}$ ,  $\log K^0 = 35.35$  at 25 °C (Watt et al., 1965), where the large equilibrium constant indicates a strong affinity to form the complex. At sufficiently high concentrations, ferrocyanides precipitate from solution as a variety of insoluble and highly soluble salts (Williams, 1915). Ferrocyanides may release free cyanide needed for prebiotic chemistry via UV light, thermal decomposition, or reactions with hydrogen sulfide (Arrhenius et al., 1994; Keefe and Miller, 1996; Patel et al., 2015). In particular, highly soluble Na/K ferrocyanide salts thermally decompose to form copious Na/K cyanide (Patel et al., 2015).

Keefe and Miller (1996) investigated ferrocyanide formation on the early Earth; however, their model is limited to dilute solutions and low ferrocyanide concentrations, and did not include solid phases or environmental factors, such as carbonate chemistry, that would have influenced ferrocyanide formation. Consequently, it is unknown if soluble ferrocyanides (e.g., Na/K/Ca/Mg ferrocyanides) could have formed, and if so, in what specific depositional environments. To address these issues, we develop a novel geochemical model for ferrocyanide-rich brines using new experimental data that includes environmental factors such as atmospheric  $\text{CO}_2$  and solution alkalinity, and accounts for solid phase carbonate, chloride, and ferrocyanide salts (Supplementary Material, Appendix B). We then use this model to explore ferrocyanide formation on the early Earth and the implications for prebiotic cyanide chemistry (Sections 3 and 4).

## 2. METHODS

### 2.1. Geochemical model

We use the Pitzer model (Pitzer, 1991) to explore how cyanides speciate and accumulate in plausible early Earth environments and which salts should precipitate. The Pitzer model accounts for ionic interactions and salt formation in concentrated brines, and has proven useful for predicting evaporating solution chemistry and salt precipitation sequences. As the basis for our Pitzer model, we use FREZCHEM (Marion and Kargel, 2008), which we implement using the *frezchem.dat* database in the geochemical program PHREEQC. PHREEQC is a freeware, user-friendly model archived by the US Geological Survey that includes aqueous equilibria (specifically, the Pitzer equations), as well as gas-phase and mineral precipitation reactions (Appelo and Postma, 2005). The *frezchem.dat* database in PHREEQC includes FREZCHEM parameters up to version 7.2, but does not contain  $\text{Fe}^{2+}$  parameters. As a result, we have supplemented *frezchem.dat* by adding Pitzer parameters and solubility products for  $\text{Fe}^{2+}$  salts from version 8.3 of FREZCHEM (Marion et al., 2003).

We also supplement *frezchem.dat* with parameters for ferrocyanide salts and ferrocyanide mixtures determined using experimental data we have gathered and literature data (Supplementary Material, Appendix B). At a minimum, parameterizing a Pitzer model requires measurements of ion activity coefficients for the pure salt phases present. Because data were not available even at 25 °C for  $\text{Na}_4\text{Fe}(\text{CN})_6$ ,  $\text{Mg}_2\text{Fe}(\text{CN})_6$ , and  $\text{Ca}_2\text{Fe}(\text{CN})_6$  salts, we measured water activities in these solutions using the isopiestic method to near saturation (Platford, 1979). Ferrocyanide solid phases in the model include  $\text{Na}_4\text{Fe}(\text{CN})_6 \cdot 10\text{H}_2\text{O}$ ,  $\text{K}_4\text{Fe}(\text{CN})_6 \cdot 3\text{H}_2\text{O}$ ,  $\text{Ca}_2\text{Fe}(\text{CN})_6 \cdot 11\text{H}_2\text{O}$ ,  $\text{Fe}_2[\text{Fe}(\text{CN})_6]$ ,  $\text{CaK}_2\text{Fe}(\text{CN})_6$ , and  $\text{MgK}_2\text{Fe}(\text{CN})_6$ . The resulting PHREEQC program used in this study is given in Supplementary Material, Appendix C.

### 2.2. Modeled environmental conditions

To constrain environmental conditions in our model, we need estimates of atmospheric HCN and  $\text{CO}_2$  concentrations on the early Earth, as well as surface water temperatures. For atmospheric  $\text{CO}_2$  levels on the early Earth, we use a range of values from 0.01 to 1 bar  $\text{CO}_2$  from Krissansen-Totton et al. (2018), who simulated  $\text{CO}_2$  by systematically varying data-constrained parameters for continental and seafloor weathering, internal heat flow and outgassing history, and greenhouse gas levels. Similarly, we use a temperature range of 0 to 25 °C, which spans the lower end of plausible surface temperatures from Krissansen-Totton et al. (2018) (0–40 °C with land and 0–50 °C without any land). We did not model temperatures above 25 °C because ferrocyanide accumulation preferentially occurs at lower temperatures (Keefe and Miller, 1996).

For the HCN gas concentrations, estimates from high-temperature models of asteroid impacts range from  $10^{-3}$  to  $10^{-5}$  bar pHCN formed locally near impact sites, to  $10^{-5}$  to  $10^{-12}$  bar pHCN distributed globally (Fegley et al., 1986). HCN deposition rates following asteroid impacts are several orders of magnitude larger than photochemical production rates (Parkos et al., 2018). Predictions of photochemical models have a similarly wide range, from  $\sim 10^{-4}$  bar pHCN in the case of high  $\text{CH}_4$  concentrations, to  $\sim 10^{-8}$  in the case of low  $\text{CH}_4$  concentrations (Zahnle, 1986; Tian et al., 2011). We use a pHCN range of  $10^{-8}$  to  $10^{-5}$  bar in our model. We note that the photochemical and asteroid impact studies referenced above show that HCN production occurs in weakly reducing  $\text{CO}_2/\text{N}_2/\text{H}_2\text{O}$ -rich atmospheres, and does not require a highly reduced atmosphere.

## 3. RESULTS

### 3.1. Ferrocyanide formation on the early Earth

Cyanide inputs to surface environments on the early Earth would have been in the form of HCN gas, which dissociates to free  $\text{CN}^-$  in aqueous solutions ( $\text{p}K_a = 9.2$  at 25 °C). This  $\text{CN}^-$  then combines with  $\text{Fe}^{2+}$  to form ferrocyanide; consequently, ferrocyanide formation depends

on aqueous  $\text{Fe}^{2+}$ ,  $\text{CN}^-$ , and  $\text{HCN}^0$  speciation. To see how these species vary as a function of pH, we model  $\text{Fe}^{2+}$ -rich solutions in equilibrium with  $\text{HCN}$  gas (Fig. 1). We find that insufficient cyanide is present as  $\text{CN}^-$  at low pH to drive ferrocyanide formation forward. As the pH increases, ferrocyanide rapidly forms over a narrow pH range as  $\text{HCN}^0$  dissociates to  $\text{CN}^-$ . In particular, we find that the pH at which  $\text{Fe}(\text{CN})_6^{4-} = \text{Fe}^{2+}$  (the equivalence point) is a useful threshold pH for evaluating the potential for ferrocyanide brines to form. Below this pH, ferrocyanide is minor, whereas above this pH, high ferrocyanide concentrations are possible.

Fig. 1 is merely an example with a specific pHCN and fixed total iron without considering Fe-containing minerals that might precipitate, so we need to investigate a broader range of plausible conditions to find the pH range in natural waters at which considerable ferrocyanide exists. To determine how the pH of the  $\text{Fe}(\text{CN})_6^{4-} = \text{Fe}^{2+}$  equivalence point changes as a function of  $p\text{CO}_2$ , pHCN, and temperature, we start with an initial solution of 0.1 mM  $\text{Fe}^{2+}$  based on modeled Archean surface waters (Hao et al., 2017), and then titrate with  $\text{Na}_2\text{CO}_3$  alkalinity until the pH of the  $\text{Fe}(\text{CN})_6^{4-} = \text{Fe}^{2+}$  equivalence point is reached (Fig. 2). The resulting pH values at the  $\text{Fe}(\text{CN})_6^{4-} = \text{Fe}^{2+}$  equivalence point are 6.9–9.3 (Fig. 2A and B), much higher than the pH of unbuffered solutions (3.8–4.9 pH), and alkalinities are  $10^{-3}$ – $2.4 \text{ mol kg}^{-1}$  in the form of bicarbonate (Fig. 2C and D).

In general, our results indicate that  $\text{Fe}(\text{CN})_6^{4-}$  is more stable at lower  $p\text{CO}_2$  and temperature, and higher pHCN. In all modeled cases, the initial aqueous  $\text{Fe}^{2+}$  precipitates as sparingly soluble siderite ( $\text{FeCO}_3$ ) or  $\text{Fe}_2[\text{Fe}(\text{CN})_6]$  (at low temperatures only), which limits the concentration of  $\text{Fe}^{2+}$  to  $10^{-9}$ – $10^{-5} \text{ mol kg}^{-1}$ . For some solutions with high  $p\text{CO}_2$  and low pHCN (the blank areas in Fig. 2), it is not possible to reach the  $\text{Fe}(\text{CN})_6^{4-} = \text{Fe}^{2+}$  equivalence point because nahcolite ( $\text{NaHCO}_3$ ) precipitates from solution, which limits the maximum possible alkalinity. As a result, such environments cannot form concentrated ferrocyanide solutions.

The previous model results indicate the minimum pH/alkalinity needed to form significant ferrocyanide in solu-

tion. Even higher ferrocyanide concentrations occur at higher pH/alkalinity, and the highest ferrocyanide concentrations occur in saturated carbonate or bicarbonate brines. Consequently, we model the highest possible ferrocyanide concentrations on the early Earth by saturating solutions with respect to  $\text{Na}_2\text{CO}_3$  alkalinity in the presence of excess  $\text{FeCO}_3$  (which supplies  $\text{Fe}^{2+}$  to solution) at variable pHCN,  $p\text{CO}_2$ , and temperature (Fig. 3). Our model results indicate that high ferrocyanide concentrations and ferrocyanide salts occur over a wide range of early Earth conditions in carbonate brines. At relatively low  $p\text{CO}_2$  and high pHCN, ferrocyanide concentrations up to  $0.7 \text{ mol kg}^{-1}$  are possible at  $25^\circ\text{C}$ ; in contrast, at relatively high  $p\text{CO}_2$  and low pHCN, cyanide is present in  $\mu\text{M}$  concentrations due to the relatively low pH and limited availability of  $\text{HCN}$  (Fig. 3E and F). The alkalinity in all cases is dominated by bicarbonate ions because the pH is buffered by acidity from  $\text{CO}_2$  and  $\text{HCN}$  gas (Fig. 3C and D).

High ferrocyanide concentrations cause  $\text{Na}_4\text{Fe}(\text{CN})_6 \cdot 10\text{H}_2\text{O}$  and  $\text{Fe}_2[\text{Fe}(\text{CN})_6]$  (Prussian White) to preferentially form at low temperatures, low  $p\text{CO}_2$ , and high pHCN, shown as “Na-Cy” and “Fe-Cy”, respectively, in Fig. 3. Solutions in the upper left regions of Fig. 3A–F are saturated with respect to nahcolite ( $\text{NaHCO}_3$ ) and siderite ( $\text{FeCO}_3$ ), but as  $p\text{CO}_2$  decreases and pHCN increases,  $\text{Na}_4\text{Fe}(\text{CN})_6 \cdot 10\text{H}_2\text{O}$  precipitates instead of nahcolite. At the lowest  $p\text{CO}_2$  and highest pHCN conditions at  $0^\circ\text{C}$ , sparingly soluble  $\text{Fe}_2[\text{Fe}(\text{CN})_6]$  precipitates in addition to  $\text{Na}_4\text{Fe}(\text{CN})_6 \cdot 10\text{H}_2\text{O}$  and siderite (Fig. 3B, D, and F). The formation of  $\text{Fe}_2[\text{Fe}(\text{CN})_6]$  is caused by high  $\text{HCN}$  gas concentrations, which leads to higher  $\text{CN}^-$  concentrations and increased iron concentrations from siderite dissolution. We note that although the solubility of  $\text{Fe}_2[\text{Fe}(\text{CN})_6]$  is poorly characterized experimentally (Supplementary Material, Appendix B), the geochemical rationale for its formation is reasonable.

### 3.2. Ferrocyanide evaporites in closed-basin lakes

Our results in the previous section show that ferrocyanide salts could have concentrated and precipitated on the early Earth in  $\text{NaHCO}_3$ -rich alkaline brines, which points to closed-basin lakes as plausible environments for

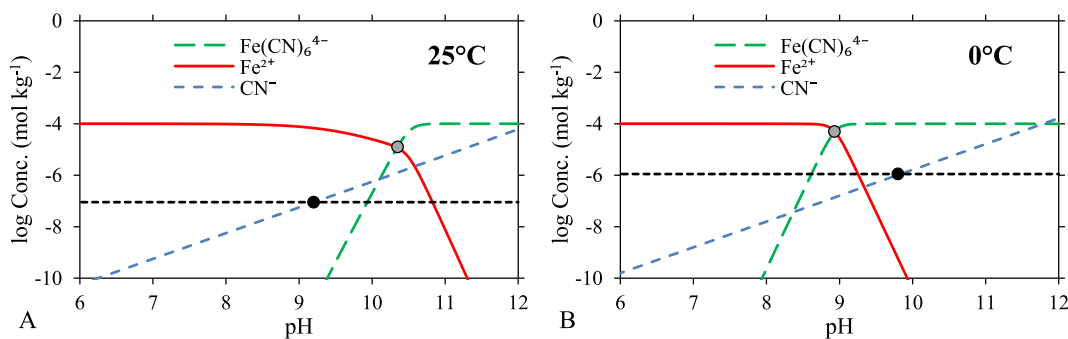


Fig. 1. Speciation in ferrocyanide solutions. Modeled solutions contain 0.1 mM total Fe in equilibrium with  $p\text{HCN} = 10^{-8}$  bar at  $25^\circ\text{C}$  (A) and  $0^\circ\text{C}$  (B) at variable pH. The  $\text{CN}^- = \text{HCN}^0$  equivalence point is indicated by black circles, and the  $\text{Fe}(\text{CN})_6^{4-} = \text{Fe}^{2+}$  equivalence point by grey circles. These equivalence points indicate a turning point in the predominance of  $\text{CN}^-$  vs.  $\text{HCN}^0$  and  $\text{Fe}(\text{CN})_6^{4-}$  vs.  $\text{Fe}^{2+}$ .

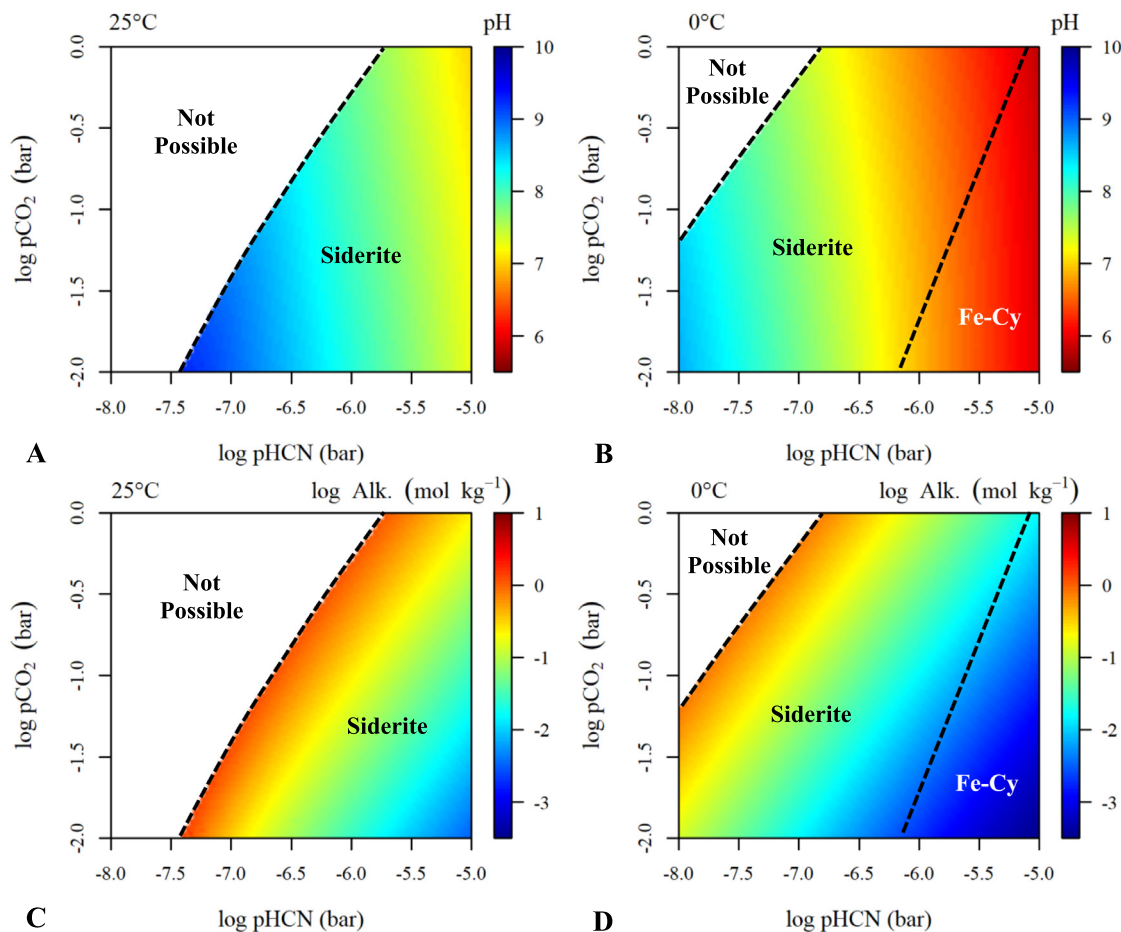


Fig. 2. The pH (A, B) and alkalinity (Alk.) (C, D) needed to form solutions in which  $\text{Fe}^{2+} = \text{Fe}(\text{CN})_6^{4-}$  at 0 and 25 °C. Solutions in the white regions are not possible (i.e.,  $\text{Fe}(\text{CN})_6^{4-} \ll \text{Fe}^{2+}$ ) because nahcolite ( $\text{NaHCO}_3$ ) precipitates, which limits the carbonate alkalinity and pH to lower values than needed to reach the  $\text{Fe}^{2+} = \text{Fe}(\text{CN})_6^{4-}$  equivalence point. Regions where siderite and  $\text{Fe}_2[\text{Fe}(\text{CN})_6]$  (designated as “(Fe-Cy)”) precipitate are delineated by dashed lines. The color scale is pH in A and B, and log alkalinity in C and D. (For interpretation of the references to colour in this figure legend, the reader is referred to the web version of this article.)

ferrocyanide accumulation. Closed-basin lakes accumulate dissolved ions from inflowing water, but have no outflow except for water loss by evaporation. Consequently, evaporation concentrates ions in lake waters to saturation, resulting in salt precipitation (Eugster and Jones, 1979). Closed-basin lakes with elevated salt concentrations are common in arid regions, and in many cases attain saturation with respect to  $\text{NaHCO}_3/\text{Na}_2\text{CO}_3$  salts (Kempe and Kazmierczak, 2011; Pecoraino et al., 2015).

To determine if closed-basin evaporation of early Earth surface water inputs could precipitate ferrocyanide salts, we model surface water evaporation at 25 °C in equilibrium with  $10^{-5}$  bar pHCN and 0.1 bar pCO<sub>2</sub> (Fig. 4). For the surface water input to the closed-basin lake, we use the Archean modeled composition from Hao et al. (2017), and achieve charge balance by adjusting  $\text{Cl}^-$ :  $\text{Na}^+ = 0.187$ ,  $\text{K}^+ = 0.0331$ ,  $\text{Ca}^{2+} = 0.226$ ,  $\text{Mg}^{2+} = 0.191$ ,  $\text{Fe}^{2+} = 0.112$ ,  $\text{Cl}^- = 0.169$ , and Alk. = 1.109 mM. This surface water composition does not include  $\text{SO}_4^{2-}$ , but sulfate salts

will not significantly affect the evaporative concentration of ferrocyanide because they accumulate at lower concentrations relative to more soluble chloride salts and do not form salts with ferrocyanide.

As evaporation of this surface water input proceeds, the alkalinity increases, raising the pH and causing the precipitation of carbonate salts in the order siderite, calcite ( $\text{CaCO}_3$ ), and  $\text{MgCO}_3$ . At the lowest residual water contents,  $\text{Na}_4\text{Fe}(\text{CN})_6 \cdot 10\text{H}_2\text{O}$  precipitates, followed by halite ( $\text{NaCl}$ ) and sylvite ( $\text{KCl}$ ) as the final salt. The final brine contains  $0.07 \text{ mol kg}^{-1} \text{ Fe}(\text{CN})_6^{4-}$ , which can be compared to ferrocyanide concentrations of  $0.68 \text{ mol kg}^{-1}$  in pure  $\text{Na}_4\text{Fe}(\text{CN})_6$  solutions. The low solubility of  $\text{Na}_4\text{Fe}(\text{CN})_6 \cdot 10\text{H}_2\text{O}$  in brine mixtures indicates a strong tendency to precipitate ferrocyanide salts in saline lakes. Although we present results for only one set of environmental conditions here, the wider set of temperature, pHCN, and pCO<sub>2</sub> conditions favorable for ferrocyanide salts in Fig. 3 also yield ferrocyanide salts in evaporative models.

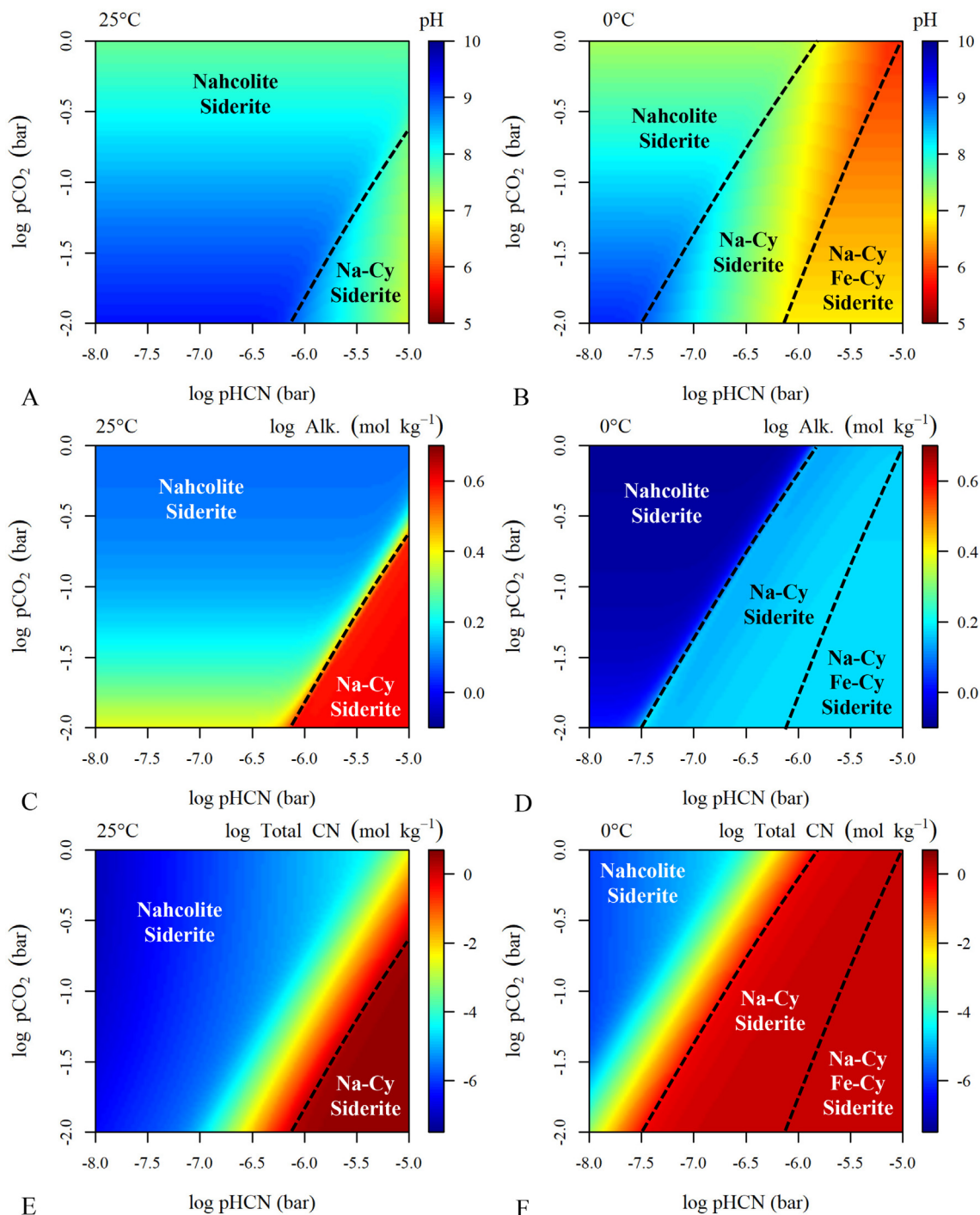


Fig. 3. Ferrocyanide concentrations in  $\text{NaHCO}_3$  brines. The modeled pH (A, B), alkalinity (C, D), and total cyanide (E, F) in solutions saturated with  $\text{Na}_2\text{CO}_3$  alkalinity at 0 and 25 °C. Regions where nahcolite, siderite,  $\text{Na}_4\text{Fe}(\text{CN})_6 \cdot 10\text{H}_2\text{O}$  (Na-Cy), and  $\text{Fe}_2[\text{Fe}(\text{CN})_6]$  (Fe-Cy) precipitate are delineated by dashed lines. Color scales are pH in A and B,  $\log(\text{Alk.})$  in C and D, and  $\log(\text{total CN})$  in E and F. (For interpretation of the references to colour in this figure legend, the reader is referred to the web version of this article.)

## 4. DISCUSSION

### 4.1. Implications for the early Earth

Our model results point to a specific environment for concentrating cyanide needed for prebiotic chemistry: relatively

low-temperature,  $\text{NaHCO}_3$ -rich, closed-basin lakes. Closed-basin lakes provide a mechanism for accumulating cyanides across hydrologic basins via inflowing waters and evaporation. Furthermore,  $\text{NaHCO}_3$ -rich lake waters would counteract acidity from early Earth's  $\text{CO}_2$ -rich atmosphere, stabilizing aqueous cyanide as ferrocyanide in alkaline

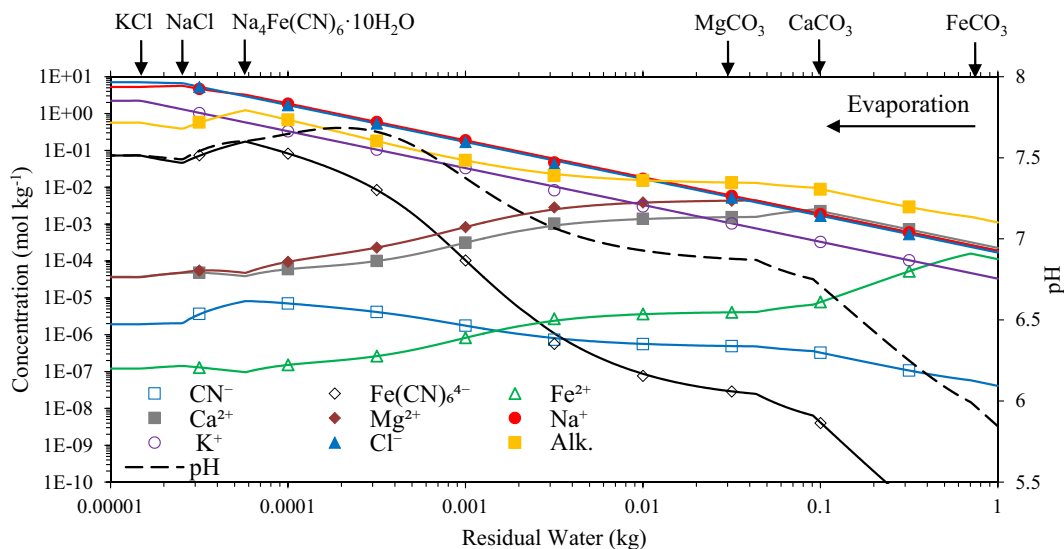


Fig. 4. Evaporative concentration of ferrocyanides. Modeled ion concentrations ( $\text{mol kg}^{-1}$ ) (solid lines) and pH (dashed line) from closed basin evaporation of Archean river water compositions in Hao et al. (2017). The initial water content of the solution is 1 kg, and the residual water is the amount of water remaining as evaporation proceeds. The initial precipitation of salt phases is indicated by arrows at the top of the graph. Evaporation proceeds from right to left, where a residual water content of 1 kg is an unevaporated solution.

solutions. Closed-basin lakes would also concentrate other potential prebiotic reagents, such as abundant carbon in the form of carbonate alkalinity, sulfur compounds, phosphates or phosphites, and trace metals (Jones et al., 1998).

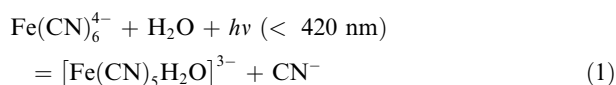
Alkaline lakes typically form in volcanic closed-basins due to chemical weathering by volcanogenic and atmospheric  $\text{CO}_2$ , which generates carbonate-rich solutions (Garrels and Mackenzie, 1967; Kempe and Kazmierczak, 2011; Pecoraino et al., 2015; Lowenstein et al., 2017). The chemistry of such lakes is determined by chemical divides (Hardie and Eugster, 1970; Eugster and Jones, 1979) and primarily depends on the relative concentrations of  $\text{Ca}^{2+} + \text{Mg}^{2+} + \text{Fe}^{2+}$  and carbonate alkalinity in the inflowing waters. Studies of present-day closed-basin lake evolution do not typically include  $\text{Fe}^{2+}$ , but in anoxic early Earth waters,  $\text{Fe}^{2+}$  would have been stable. When  $\text{Ca}^{2+} + \text{Mg}^{2+} + \text{Fe}^{2+}$  is greater than carbonate alkalinity, most of the alkalinity precipitates as insoluble carbonates, resulting in relatively low alkalinity waters (Hardie and Eugster, 1970; Eugster and Jones, 1979). In contrast, when  $\text{Ca}^{2+} + \text{Mg}^{2+} + \text{Fe}^{2+}$  is less than carbonate alkalinity, these cations are removed from evaporating waters as their carbonates and the residual lake water becomes enriched in  $\text{NaHCO}_3$ .

Closed-basin alkaline lakes are commonly found in mafic (e.g., basaltic) terrains. Experimental studies of anoxic chemical weathering of basalts (Fabre et al., 2011) in the presence of  $\text{CO}_2$  indicate that  $\text{H}^+$  is consumed (increasing the pH), carbonate alkalinity increases, and  $\text{Na}^+$  preferentially migrates into the aqueous phase relative to  $\text{Ca}^{2+}$ ,  $\text{Mg}^{2+}$ , and especially  $\text{Fe}^{2+}$ . Precipitation of secondary silicate minerals also consumes  $\text{Mg}^{2+}$ ,  $\text{Fe}^{2+}$ , and  $\text{K}^+$  ions, leading to an overall condition of  $\text{Ca}^{2+} + \text{Mg}^{2+} + \text{Fe}^{2+} < \text{carbonate alkalinity}$ . In addition, chemical weathering of mafic minerals such as olivine and pyroxene, as

well as glass abundant in mafic rocks, is relatively rapid (Gislason and Hans, 1987; Gudbrandsson et al., 2011), leading to high fluxes of carbonate alkalinity to closed-basin lakes. Upon evaporation, such inflow waters evolve to  $\text{NaHCO}_3$ -rich brines.

On the early Earth, mafic and ultramafic rocks were common and fresh volcanic material would have been abundant due to active early volcanism (Taylor and McLennan, 1995). Furthermore, landmasses may have been present as early as the Hadean based on evidence from zircons (Harrison, 2009), possibly associated with hotspot volcanism (Bada and Korenaga, 2018), and there is strong evidence for landmasses in the early Archean based on  $\sim 3.8$  Ga sediments in Greenland (Nutman et al., 1997; Viehmann, 2018). Chemical weathering of such landmasses in Earth's relatively high  $\text{CO}_2$  environment (Zahnle et al., 2010) would have released alkali cations and formed alkaline waters, which upon evaporation in closed-basin settings would have formed  $\text{NaHCO}_3$ -rich lakes. Such alkaline lake environments are inferred to have been preserved in the Archean geologic record in the Ventersdorp and Tumbiana formations (Karpeta, 1989; Stüeken et al., 2015), and may have been abundant in the early Archean and Hadean also.

A potential complication is that ultraviolet light (UV) may decompose ferrocyanide in the lake through aqueous photochemical dissociation (Broderius and Smith, 1980). Ferrocyanide absorbs UV wavelengths less than 420 nm, resulting in the rapid formation of an unstable  $[\text{Fe}(\text{CN})_5\text{H}_2\text{O}]^{3-}$  complex and free  $\text{CN}^-$ :



If ferrocyanide solutions were exposed on Earth's surface, this reaction would likely have been important because of a greater flux of near-UV radiation caused by the absence of a stratospheric ozone layer on the early Earth (Catling and Kasting, 2017; p. 291).

Although photodecomposition of ferrocyanide via reaction (13) is expected to produce free cyanide as HCN or  $\text{CN}^-$ , it can only form extremely low concentrations of free cyanide because of a rapid back reaction. For example, Åsperg er (1952) found that exposing 75 mM ferrocyanide solutions (the concentration at which ferrocyanide precipitates in our evaporative model in Fig. 4) to UV light from a mercury lamp only decomposes  $\sim 0.005\%$  of the ferrocyanide after several hours of irradiation, and that decomposition completely reverses in the dark. Furthermore, reaction (13) increases the solution pH, which inhibits the formation of HCN, resulting in negligible HCN losses to the atmosphere (Åsperg er, 1952). Even if HCN were released during the daytime, it would redissolve in aqueous environments during the nighttime (Keefe and Miller, 1996).

Alkaline closed-basin lakes could have concentrated atmospheric HCN as aqueous and solid phase ferrocyanides, but prebiotic synthesis schemes require free cyanide in the form of  $\text{HCN}^0$  or  $\text{CN}^-$ . Patel et al. (2015) qualitatively hypothesized that free cyanide could have been released in quantity by thermal decomposition of ferrocyanide salt evaporites, possibly via magmatic activity or thermal shock from asteroid impact events. The cationic form of the ferrocyanide salt is important because the thermal decomposition products differ depending on the cation (Patel et al., 2015). Na and K-ferrocyanides decompose to NaCN and KCN respectively, and the iron is sequestered as insoluble iron carbide, which does not recombine to form ferrocyanide if water is added.  $\text{Mg}_2\text{Fe}(\text{CN})_6$  decomposes to magnesium nitride ( $\text{Mg}_3\text{N}_2$ ), and  $\text{Ca}_2\text{Fe}(\text{CN})_6$  decomposes to calcium cyanamide ( $\text{CaNCN}$ ) and calcium carbide ( $\text{CaC}_2$ ). Such thermal decomposition products can act as key reagents in prebiotic organic synthesis schemes (Patel et al., 2015; Ritson et al., 2018). The thermal decomposition of  $\text{Fe}_2[\text{Fe}(\text{CN})_6]$  has not been studied, but the likely solid phase decomposition products are iron carbide and carbon, which have no special significance for organic synthesis.

Our model predicts the new finding that only  $\text{Na}_4\text{Fe}(\text{CN})_6 \cdot 10\text{H}_2\text{O}$  and  $\text{Fe}_2[\text{Fe}(\text{CN})_6]$  would have formed in early Earth environments, which suggests that thermal decomposition would have yielded only NaCN for prebiotic synthesis. Ca and Mg-ferrocyanides would not form because concentrated ferrocyanides only accumulate in highly alkaline brines, which precipitate  $\text{Ca}^{2+}$  and  $\text{Mg}^{2+}$  ions as carbonates.  $\text{K}_4\text{Fe}(\text{CN})_6 \cdot 3\text{H}_2\text{O}$  is also unlikely because it is more soluble than  $\text{Na}_4\text{Fe}(\text{CN})_6 \cdot 10\text{H}_2\text{O}$ , and granitoid continental rocks on the early Earth have low K/Na ratios compared to modern granites (Condie, 1993), so the source rocks for weathering fluids and river input should be relatively K-poor. Finally, our model does not predict the formation of sparingly soluble ferrocyanide compounds such as  $\text{CaK}_2\text{Fe}(\text{CN})_6$  and  $\text{MgK}_2\text{Fe}(\text{CN})_6$ .

Thermal decomposition would have acted on the other phases in evaporite sequences, along with sedimentary  $\text{Na}_4\text{Fe}(\text{CN})_6 \cdot 10\text{H}_2\text{O}$ . Based on our closed-basin model

(Fig. 4), the other phases should be Ca/Mg/Fe carbonates, nahcolite, halite, and sylvite, as well as possibly sulfates (not modeled here).  $\text{CaCO}_3$  decomposes to CaO at  $\sim 800^\circ\text{C}$ , whereas Mg and Fe carbonates decompose to their oxides at  $400\text{--}500^\circ\text{C}$  (Stern and Weise, 1969). In contrast, Na/K chlorides and  $\text{Na}_2\text{CO}_3$  (the dehydration product of  $\text{NaHCO}_3$ ) are stable to very high temperatures. Although we consider decomposition of single phases here, we note that decomposition may have occurred in salt mixtures, which could alter the decomposition temperatures and products. The addition of water to likely thermal decomposition compounds, via surface or groundwater flows, would hydrate the oxides to hydroxides, and form alkaline solutions due to Ca/Mg/Fe hydroxide and  $\text{Na}_2\text{CO}_3$  dissolution. These decomposition products, although not necessary for the formation of aqueous NaCN, are compatible with alkaline NaCN solutions.

An alkaline NaCN-rich flow can also provide other essential chemical species needed for prebiotic chemistry (Patel et al., 2015). Reactions with pyrite, a common crustal mineral, would release thiocyanate ( $\text{SCN}^-$ ) and bisulfide ( $\text{HS}^-$ ), which can act as a reducing agent to build organic molecules from cyanide derivatives in photoredox reactions. Vivianite ( $\text{Fe}_2(\text{PO}_4)_3 \cdot 8\text{H}_2\text{O}$ ) derived from weathered meteoric material could dissolve to form ferrocyanide and release phosphate, a key component of nucleotides (Patel et al., 2015). Phosphate could also concentrate by evaporation, driving its reactions. Copper (II) sulfides would react to form bisulfide, as well as copper (I) cyanide ( $\text{CuCN}$ ), a potential catalyst for prebiotic chemistry, and cyanogen gas ( $\text{C}_2\text{N}_2$ ), a compound implicated in the formation of cytosine (Shapiro, 1999). Hence, a variety of prebiotic ingredients are possible via the interaction of aqueous NaCN with crustal minerals.

Our model does not predict the formation of  $\text{Ca}_2\text{Fe}(\text{CN})_6$ , which thermally decomposes to CaNCN, a component in the formation of pyrimidines in prebiotic synthesis schemes (Ritson et al., 2018). In the evaporite model (Fig. 4), calcium is removed from alkaline solutions by calcite precipitation. Consequently, cyanamide would need to form via a different geochemical pathway. Another possible route for calcium cyanamide synthesis is by the reaction of CaO (derived from thermal decomposition of  $\text{CaCO}_3$ ) with nitrogen compounds under reducing conditions (G uthner and Mertschenk, 2006). For example, CaNCN could form by post-impact heating of  $\text{CaCO}_3$  if the atmosphere were temporarily enriched in HCN, or in CO and  $\text{NH}_3$ .

## 5. CONCLUSIONS

The results presented here show that high ferrocyanide concentrations and  $\text{Na}_4\text{Fe}(\text{CN})_6 \cdot 10\text{H}_2\text{O}$  and/or  $\text{Fe}_2[\text{Fe}(\text{CN})_6]$  salts were possible on the early Earth over a wide and plausible range of temperature,  $p\text{CO}_2$ , and  $p\text{HCN}$ . Ferrocyanide salts could have formed in closed-basin  $\text{NaHCO}_3$ -rich lakes, which would have been common on the early Earth due to high atmospheric  $\text{CO}_2$  and active mafic volcanism. Evaporite salt assemblages containing ferrocyanides could have thermally decomposed to NaCN, as well as Ca/Mg/Fe oxides and  $\text{Na}_2\text{CO}_3$ , which dissolve in aqueous

solution to form NaCN-rich solutions. This free cyanide could then have participated in prebiotic reactions. These results provide a rigorous geochemical pathway for the formation of concentrated, free cyanide, and suggest a specific environment in alkaline, closed-basin lakes. The results also indicate a specific nucleophile, NaCN, for prebiotic synthesis. Such a prebiotic lake environment may also be important for consideration of life originating on other planets, such as Mars.

#### ACKNOWLEDGEMENTS

Funding was provided by the Simons Collaboration on the Origin of Life grant 511570 awarded to DCC. We thank John Sutherland for useful discussions.

#### APPENDIX A. SUPPLEMENTARY MATERIAL

Supplementary data to this article can be found online at <https://doi.org/10.1016/j.gca.2019.06.031>.

#### REFERENCES

- Appelo C. A. J. and Postma D. (2005) *Geochemistry, Groundwater and Pollution*, second ed. CRC Press, Boca Raton, FL.
- Arrhenius T., Arrhenius G. and Paplawsky W. (1994) Archean geochemistry of formaldehyde and cyanide and the oligomerization of cyanohydrin. *Origins Life Evol. Biosphere* **24**, 1–17.
- Ašperger S. (1952) Kinetics of the decomposition of potassium ferrocyanide in ultra-violet light. *Trans. Faraday Soc.* **48**, 617–624.
- Bada J. and Korenaga J. (2018) Exposed areas above sea level on Earth > 3.5 Gyr ago: implications for prebiotic and primitive biotic chemistry. *Life* **8**, 1–9.
- Broderius, S. J. and Smith, L. L. (1980) Direct photolysis of hexacyanoferrate complexes: proposed applications to the aquatic environment.
- Catling D. C. and Kasting J. F. (2017) *Atmospheric Evolution on Inhabited and Lifeless Worlds*. Cambridge University Press, Cambridge, UK.
- Cleaves H. J., Chalmers J. H., Lazcano A., Miller S. L. and Bada J. L. (2008) A reassessment of prebiotic organic synthesis in neutral planetary atmospheres. *Origins Life Evol. Biospheres* **38**, 105–115.
- Condie K. C. (1993) Chemical composition and evolution of the upper continental crust: contrasting results from surface samples and shales. *Chem. Geol.* **104**, 1–37.
- Eugster H. P. and Jones B. F. (1979) Behavior of major solutes during closed-basin brine evolution. *Am. J. Sci.* **279**, 609–631.
- Fabre S., Berger G. and Nédélec A. (2011) Modeling of continental weathering under high-CO<sub>2</sub> atmospheres during Precambrian times. *Geochem. Geophys. Geosyst.* **12**, 1–23.
- Fegley, Jr, B., Prinn R. G., Hartman H. and Watkins G. H. (1986) Chemical effects of large impacts on the Earth's primitive atmosphere. *Nature* **319**, 305–308.
- Ferris J. P. and Hagan, Jr, W. J. (1984) HCN and chemical evolution: the possible role of cyano compounds in prebiotic synthesis. *Tetrahedron* **40**, 1093–1120.
- Ferus M., Kubelík P., Knížek A., Pastorek A., Sutherland J. and Civiš S. (2017) High energy radical chemistry formation of HCN-rich atmospheres on early Earth. *Sci. Rep.* **7**, 1–9.
- Garrels R. M. and Mackenzie F. T. (1967) Origin of the chemical compositions of some springs and lakes. *Equilib. Concepts Nat. Water Syst.*, 222–242.
- Gislason S. R. and Hans P. E. (1987) Meteoric water-basalt interactions. I: A laboratory study. *Geochim. Cosmochim. Acta* **51**, 2827–2840.
- Gudbrandsson S., Wolff-Boenisch D., Gislason S. R. and Oelkers E. H. (2011) An experimental study of crystalline basalt dissolution from 2 < pH < 11 and temperatures from 5 to 75°C. *Geochim. Cosmochim. Acta* **75**, 5496–5509.
- Güthner T. and Mertschenk B. (2006) *Cyanamides, Ullmann's encyclopedia of industrial chemistry*. Wiley-VCH Verlag GmbH & Co., pp. 645–667.
- Hao J., Sverjensky D. A. and Hazen R. M. (2017) A model for late Archean chemical weathering and world average river water. *Earth. Planet. Sci. Lett.* **457**, 191–203.
- Hardie L. H. and Eugster H. P. (1970) The evolution of closed-basin brines. *Mineral. Soc. Am. Spec. Pap.* **3**, 273–290.
- Harrison T. M. (2009) The Hadean crust: evidence from > 4 Ga zircons. *AREPS* **37**, 479–505.
- Jones B. E., Grant W. D., Duckworth A. W. and Owenson G. G. (1998) Microbial diversity of soda lakes. *Extremophiles* **2**, 191–200.
- Karpeta W. P. (1989) Bedded cherts in the Rietgat Formation, Hartbeesfontein, South Africa: a late Archean to early Proterozoic magadiitic alkaline playa lake deposit? *S. Afr. J. Geol.* **92**, 29–36.
- Keefe A. D. and Miller S. L. (1996) Was ferrocyanide a prebiotic reagent? *Origins Life Evol. Biosphere* **26**, 111–129.
- Kempe, S. and Kazmierczak, J. (2011) Soda lakes. In: (eds. J., R., V., T), *Encyclopedia of Geobiology*. Springer, Dordrecht, pp. 824–829.
- Krissansen-Totton J., Arney G. N. and Catling D. C. (2018) Constraining the climate and ocean pH of the early Earth with a geological carbon cycle model. *Proc. Natl. Acad. Sci.* **115**, 4105–4110.
- Lowenstein T. K., Jagniecki E. A., Carroll A. R., Smith M. E., Renaut R. W. and Owen R. B. (2017) The Green River salt mystery: what was the source of the hyperalkaline lake waters? *Earth Sci. Rev.* **173**, 295–306.
- Marion G. M., Catling D. C. and Kargel J. S. (2003) Modeling aqueous ferrous iron chemistry at low temperatures with application to Mars. *Geochim. Cosmochim. Acta* **67**, 4251–4266.
- Marion G. M. and Kargel J. S. (2008) *Cold Aqueous Planetary Geochemistry with FREZCHEM: From Modeling to the Search for Life at the Limits*. Springer, Berlin/Heidelberg.
- Matthews C. N. and Minard R. D. (2006) Hydrogen cyanide polymers, comets and the origin of life. *Faraday Discuss.* **133**, 393–401.
- Miller S. L. and Orgel L. E. (1974) *The Origins of Life on the Earth (Concepts of Modern Biology)*. Prentice Hall, Englewood Cliffs, NJ.
- Miyakawa S., Cleaves H. J. and Miller S. L. (2002) The cold origin of life: A. Implications based on the hydrolytic stabilities of hydrogen cyanide and formamide. *Origins Life Evol. Biosphere* **32**, 195–208.
- Nutman A. P., Mojzsis S. J. and Friend C. R. (1997) Recognition of ≥3850 Ma water-lain sediments in West Greenland and their significance for the early Archean Earth. *Geochim. Cosmochim. Acta* **61**, 2475–2484.
- Parkos D., Pikus A., Alexeenko A. and Melosh H. J. (2018) HCN production via impact ejecta reentry during the Late Heavy Bombardment. *J. Geophys. Res. Planets* **123**, 892–909.
- Patel B. H., Percivalle C., Ritson D. J., Duffy C. D. and Sutherland J. D. (2015) Common origins of RNA, protein and lipid precursors in a cyanosulfidic protometabolism. *Nat. Chem.* **7**, 301–307.

- Pecoraino G., D'Alessandro W. and Inguaggiato S. (2015) *The Other Side of the Coin: Geochemistry of Alkaline Lakes in Volcanic Areas*. Volcanic Lakes. Springer, Berlin, Heidelberg, pp. 219–237.
- Pitzer K. S. (1991) Ion interaction approach: Theory and data correlation. In *Activity Coefficients in Electrolyte Solutions*, second ed. CRC Press, Boca Raton, pp. 75–153.
- Platford R. F. (1979) Experimental methods: isopiestic. In *Activity Coefficients in Electrolyte Solutions* (ed. R. M. Pytkowicz). CRC Press Inc, Boca Raton, FL.
- Ritson D. J., Battilocchio C., Ley S. V. and Sutherland J. D. (2018) Mimicking the surface and prebiotic chemistry of early Earth using flow chemistry. *Nat. Commun.* **9**, 1–10.
- Sanchez R. A., Ferbis J. P. and Orgel L. E. (1967) Studies in Prebiotic Synthesis: II. Synthesis of purine precursors and amino acids from aqueous hydrogen cyanide. *J. Mol. Biol.* **30**, 223–253.
- Schlesinger G. and Miller S. L. (1973) Equilibrium and kinetics of glyconitrile formation in aqueous solution. *J. Am. Chem. Soc.* **95**, 3729–3735.
- Shapiro R. (1999) Prebiotic cytosine synthesis: a critical analysis and implications for the origin of life. *Proc. Natl. Acad. Sci.* **96**, 4396–4401.
- Shtyrlin V. G., Borissenok V. A., Serov N. Y., Simakov V. G., Bragunets V. A., Trunin I. R., Tereshkina I. A., Koshkin S. A., Bukharov M. S., Gilyazetdinov E. M. and Shestakov E. E. (2019) Prebiotic syntheses under shock in the water–formamide–potassium bicarbonate–sodium hydroxide system. *Origins Life Evol. Biospheres*, 1–18.
- Stern K. H. and Weise E. L. (1969) High temperature properties and decomposition of inorganic salts. Part 2 Carbonates. *Natl. Standard Data Ref. Syst.*, 1–27.
- Stribling R. and Miller S. L. (1987) Energy yields for hydrogen cyanide and formaldehyde syntheses: the HCN and amino acid concentrations in the primitive ocean. *Origins Life Evol. Biosphere* **17**, 261–273.
- Stüeken E. E., Buick R. and Schauer A. J. (2015) Nitrogen isotope evidence for alkaline lakes on late Archean continents. *Earth. Planet. Sci. Lett.* **411**, 1–10.
- Taylor S. R. and McLennan S. M. (1995) The geochemical evolution of the continental crust. *Rev. Geophys.* **33**, 241–265.
- Tian F., Kasting J. F. and Zahnle K. (2011) Revisiting HCN formation in Earth's early atmosphere. *Earth. Planet. Sci. Lett.* **208**, 417–423.
- Viehmann S. (2018) Hf-Nd isotopes in archean marine chemical sediments: implications for the geodynamical history of early earth and its impact on earliest marine habitats. *Geosciences* **8**, 1–15.
- Watt G. D., Christensen J. J. and Izatt R. M. (1965) Thermodynamics of metal cyanide coordination. III.  $\Delta G^\circ$ ,  $\Delta H^\circ$ , and  $\Delta S^\circ$  values for ferrocyanide and ferricyanide ion formation in aqueous solution at 25°. *Inorg. Chem.* **4**, 220–222.
- Williams H. E. (1915) *The Chemistry of Cyanogen Compounds and their Manufacture and Estimation*. J. & A Churchill, London.
- Zahnle K., Schaefer L. and Fegley B. (2010) Earth's earliest atmospheres. *Cold Spring Harbor Perspect. Biol.* **2**, 1–18.
- Zahnle K. J. (1986) Photochemistry of methane and the formation of hydrocyanic acid (HCN) in the Earth's early atmosphere. *J. Geophys. Res.: Atmos.* **91**, 2819–2834.

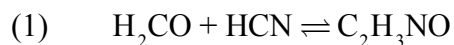
Associate editor: Nicholas Tosca

## Supplementary Material

### 1. Appendix A: Potential competing reactions for HCN

There are several reactions not included in our model that can consume HCN produced on the early Earth, which could limit the formation of ferrocyanide. We briefly consider three such reactions here: (1) the reaction of formaldehyde ( $\text{H}_2\text{CO}$ ) with HCN to produce glyconitrile ( $\text{C}_2\text{H}_3\text{NO}$ ), (2) the hydrolysis of HCN to formamide ( $\text{H}_3\text{CNO}$ ), and (3) the irreversible reaction of HCN with elemental sulfur or polysulfides to produce thiocyanate ions ( $\text{SCN}^-$ ).

HCN reacts with formaldehyde to form glyconitrile as follows:



where the equilibrium constant for this reaction is  $4.6 \times 10^6$ , indicating a strong preference for glyconitrile formation (Schlesinger and Miller, 1973). This suggests that HCN accumulation in surface environments requires a greater HCN production rate relative to formaldehyde; although, formaldehyde could potentially be consumed by many other reactions (Cleaves II, 2008). Photochemical models of early Earth's atmosphere suggest that HCN production is greater than formaldehyde only at relative high methane mixing ratios in the atmosphere (Zahnle, 1986). On the other hand, asteroid impacts are predicted to produce orders of magnitude more HCN than formaldehyde (Fegley Jr et al., 1986), in which case excess HCN would remain after consumption by formaldehyde.

Another pathway for HCN destruction is slow hydrolysis to formamide in aqueous solutions, which then further hydrolyzes to formic acid (Miyakawa et al., 2002). The ocean could act as a sink for HCN through dissolution and hydrolysis to formaldehyde, which may have limited the atmospheric HCN concentration available to closed-basin lake environments. Using experimental measurements of pH-dependent hydrolysis rates, Miyakawa et al. (2002) estimated that the steady state concentration of HCN in the ocean would have been  $2 \times 10^{-6}$  M at a temperature of  $0^\circ\text{C}$ , ocean pH = 8, and assuming a HCN deposition rate of  $2 \times 10^9$  molecules  $\text{cm}^{-2} \text{s}^{-1}$ . If the ocean is in equilibrium with the atmosphere, this translates to  $\text{pHCN} = 10^{-8}$  bar using the Henry Law constant, which is the lowest pHCN value that we consider in our model. However, asteroid impacts can result in HCN production rates three orders of magnitude greater (Fegley Jr et al., 1986; Parkos et al., 2018) than assumed in Miyakawa et al. (2002). Given that the steady state HCN concentration in the ocean scales linearly with the production rate, an increase in the HCN production rate by a factor of  $10^3$  results in  $\text{pHCN} = 10^{-5}$  bar, which is the highest value of pHCN that we consider in our model.

Finally, we consider the irreversible and rapid reaction of HCN with elemental sulfur and polysulfide species to form thiocyanates (Luthy and Bruce Jr, 1979). HCN accumulation on early Earth would only be plausible if the HCN deposition flux to surface environments exceeded that of sulfur species, with the exception of  $\text{H}_2\text{S}$ , which does not react with cyanide. The photochemical model of Zahnle et al. (2006) indicates that elemental sulfur is produced from volcanic gases, and is enhanced at low  $\text{O}_2$  and high  $\text{CH}_4$  mixing ratios. For favorable  $\text{O}_2$  and  $\text{CH}_4$  mixing ratios, the nominal flux of elemental sulfur is  $\sim 10^9$  molecules  $\text{cm}^{-2} \text{s}^{-1}$ . Given that HCN production rates can

exceed this value, especially during asteroid impacts, we conclude that the accumulation of HCN in surface environments is plausible.

## **2. Appendix B: Experimental methods, results, and model development**

### **2.1. Materials**

Ferrocyanide salt solutions were prepared by diluting  $\text{Na}_4\text{Fe}(\text{CN})_6$ ,  $\text{Mg}_2\text{Fe}(\text{CN})_6$ , and  $\text{Ca}_2\text{Fe}(\text{CN})_6$  stock solutions. We used NaCl as the reference solution for the isopiestic method described in the second section below. The NaCl and  $\text{Na}_4\text{Fe}(\text{CN})_6$  salts were purchased from online supplies, whereas we synthesized the  $\text{Mg}_2\text{Fe}(\text{CN})_6$  and  $\text{Ca}_2\text{Fe}(\text{CN})_6$  salts from  $\text{Ba}_2\text{Fe}(\text{CN})_6$ .  $\text{Ba}_2\text{Fe}(\text{CN})_6$  was prepared by mixing saturated solutions of  $\text{Na}_4\text{Fe}(\text{CN})_6$  and  $\text{BaCl}_2$ , which precipitates  $\text{Ba}_2\text{Fe}(\text{CN})_6$  as a sparingly soluble salt. The  $\text{Ba}_2\text{Fe}(\text{CN})_6$  was then washed with deionized water until the supernatant was free of  $\text{Ba}^{2+}$  or  $\text{Cl}^-$  salts. To prepare  $\text{Ca}_2\text{Fe}(\text{CN})_6$ , we mixed an excess of gypsum ( $\text{CaSO}_4 \cdot 2\text{H}_2\text{O}$ ) with  $\text{Ba}_2\text{Fe}(\text{CN})_6$ . The  $\text{Ba}^{2+}$  precipitates as insoluble  $\text{BaSO}_4$ , leaving behind the soluble calcium ferrocyanide salt. To prepare  $\text{Mg}_2\text{Fe}(\text{CN})_6$ , we mixed a slight excess of  $\text{MgSO}_4$  and  $\text{BaCO}_3$  with  $\text{Ba}_2\text{Fe}(\text{CN})_6$ . The  $\text{BaCO}_3$  addition combines with excess  $\text{MgSO}_4$  to precipitate insoluble  $\text{BaSO}_4$  and  $\text{MgCO}_3$  salts. We separated the resulting slurries by centrifuging and then filtering the supernatant at  $0.45 \mu\text{m}$ . Finally, we purified all salts by (1) making saturated salt solutions and (2) recrystallizing the solutions and discarding the supernatant. We then prepared near-saturated stock solutions from the residual crystals.

We measured the concentration of the NaCl stock solution gravimetrically by dehydration in a vacuum oven overnight at  $250^\circ\text{C}$  and  $0.02 \text{ mbar}$ . For the ferrocyanide solutions, dehydration leads to partial decomposition on the salt and/or the salt retains water despite extensive drying (Vallance, 1927; Williams, 1915). As a result, we measured the concentration of these solutions gravimetrically as  $\text{Fe}_2\text{O}_3$  using the following procedure. First, we acidified aliquots of the ferrocyanide solutions with concentrated  $\text{H}_2\text{SO}_4$  under a fume hood, and heated the mixture on a hot plate slowly until all the  $\text{H}_2\text{SO}_4$  evaporated at  $\sim 300^\circ\text{C}$ . This decomposes the ferrocyanide into iron sulfate salts. Completeness of decomposition could be tested by adding water to cooled samples. This precipitates Prussian blue if cyanide remains, in which case the decomposition procedure was repeated. After decomposition, samples were acidified with  $\text{HNO}_3$  and heated to boiling to oxidize  $\text{Fe}^{2+}$  to  $\text{Fe}^{3+}$ , and then neutralized with concentrated ammonia to  $\sim 7 \text{ pH}$  to precipitate iron hydroxides. We then filtered this precipitate and ignited the sample at  $950^\circ\text{C}$  to yield  $\text{Fe}_2\text{O}_3$ . Triplicate analyses of the stock solutions gave results within  $\pm 0.01$  (Table 1).

### **2.2. Water activity measurements and results**

The isopiestic method measures water activity by equilibrating an unknown solution with a reference solution over the vapor phase. Water vapor will transfer between the two solutions until the water vapor pressures over the reference and unknown solutions are equivalent, i.e. until their water activities are equivalent. The final weights after equilibration determine the amount of water transfer between the solutions, and their equilibrium concentrations. Because (1) the water activity of the reference solution is known and (2) the water activity in the reference and sample solutions are equal, this measurement determines the water activity of the sample solution as a function of concentration.

We recently developed a set of ten glass isopiestic apparatus comprised of two  $\sim 10 \text{ ml}$  glass flasks (Toner and Catling, 2018), each containing a small magnetic stir-bar ( $2 \times 7 \text{ mm}$ ) to agitate the solutions, and connected to a glass manifold via ground-glass joints using hydrocarbon-based

grease. Briefly, the experimental procedure consists of weighing solutions of known concentration into the vials, evacuating the apparatus down to 0.05 mbar, and equilibrating the samples at  $25 \pm 0.01$  °C in a water bath over a period of two to five days. Then, we weighed each solution. Platford (1979) provides a detailed description of the isopiestic method. Results from the isopiestic experiments are given in Table 2 and Fig. 1.

### 2.3. Geochemical model

To model concentrated ferrocyanide solutions, we use the Pitzer model (Pitzer, 1991). The Pitzer equation for the excess Gibbs energy of solution ( $G^{EX}$ ) in a mixed aqueous salt solution containing cations  $c$  and anions  $a$  is given by:

$$(2) \quad G^{EX} = -4A_\phi \ln(1 + b\sqrt{I}) \frac{I}{b} + \sum_c \sum_a m_c m_a (2\beta_{ca} + ZC_{ca}) + \sum_c \sum_{c'} m_c m_{c'} \left( 2\Phi_{cc'} + m_a \sum_a \psi_{cc'a} \right) + \sum_a \sum_{a'} m_a m_{a'} \left( 2\Phi_{aa'} + m_c \sum_c \psi_{aa'c} \right)$$

In this equation, subscript  $M$  indicates a cation, subscript  $X$  indicates an anion,  $c'$  is a cation different from  $c$ ,  $a'$  is an anion different from  $a$ ,  $b$  is a constant ( $1.2 \text{ kg}^{-1/2} \text{ mol}^{-1/2}$ ),  $I$  is the ionic strength given by  $I = \frac{1}{2} \sum m_i z_i^2$ ,  $z_i$  is the ion charge,  $Z$  is given by  $Z = \sum m_i |z_i|$ , and  $A_\phi$  is the Debye–Hückel limiting law slope. Differentiation of  $G^{EX}$  with respect to moles of water ( $n_1$ ) and salt ( $n_i$ ) at molality  $m$  ( $\text{mol} \cdot \text{kg}^{-1}$ ) leads to expressions for the activity coefficients for water ( $a_w$ ) and salt ( $\gamma$ ) respectively:

$$(3) \quad \frac{\partial G^{EX}}{\partial n_1} = RT \ln a_w \quad \text{and} \quad \frac{\partial G^{EX}}{\partial n_i} = RT \ln m_i \gamma_i$$

Importantly, water activities are commonly reported as osmotic coefficients ( $\phi$ ), which are related by the equation:

$$(4) \quad \phi = -55.50844 \frac{\ln a_w}{\sum m_i}$$

The parameters  $\beta$ ,  $C$ , and  $\Phi$  are given by the functions:

$$(5) \quad \beta_{ca} = \beta_{ca}^{(0)} + \beta_{ca}^{(1)} g(\alpha_1 \sqrt{I}) + \beta_{ca}^{(2)} g(\alpha_2 \sqrt{I})$$

$$(6) \quad C_{ca} = \frac{C_{ca}^\phi}{2\sqrt{|z_c z_a|}}$$

$$(7) \quad \Phi_{ij} = \theta_{ij} + {}^E \theta_{ij}$$

where  ${}^E\theta_{ij}$  is a higher-order electrostatic terms that account for interactions between ions of the same sign, but different charge (i.e.  $z_i \neq z_j$ ), and  $g(x)$  is given by:

$$(8) \quad g(x) = \frac{2[1 - (1+x)e^{-x}]}{x^2}$$

These equations indicate that the Pitzer equations describe properties in mixed electrolyte solutions using the empirical parameters  $\beta^{(0)}$ ,  $\beta^{(1)}$ ,  $\beta^{(2)}$ ,  $C^\phi$ ,  $\theta$ ,  $\psi$ ,  $\alpha_1$ , and  $\alpha_2$ . For a more complete description of the Pitzer model employed here, see Marion and Kargel (2008).

Ferrocyanides undergo extensive speciation in aqueous solutions because of the high negative charge. Aqueous chemical models deal with speciation either by (1) explicitly including aqueous complexes and their association constants in the model, or (2) treating the salt as free ions and implicitly accounting for ion association effects. The first approach is generally used for relatively dilute solutions, but for concentrated solutions relevant to the Pitzer approach (therefore relevant to this study), the second approach is used. For example,  $\text{MgSO}_4$  salts are well-known to form aqueous  $\text{MgSO}_4^0$  complexes, but Pitzer models including this salt treat it as fully dissociated  $\text{Mg}^{2+}$  and  $\text{SO}_4^{2-}$  ions (Pitzer and Mayorga, 1974). The ion activity (i.e., the effective salt concentration that controls reactions) modeled in this treatment is interpreted as a ‘‘mean ion activity’’ that implicitly incorporates the effects of any  $\text{MgSO}_4^0$  complexes. When applied to mixtures, this approach is able to accurately represent  $\text{MgSO}_4$  solubilities in mixed, concentrated salt systems (Harvie and Weare, 1980). Ferrocyanides also form ion pairs in solution, but as for the  $\text{MgSO}_4$  system, we treat the ferrocyanides as fully dissociated electrolytes, and implicitly account for ion pairing effects in our ion activity model.

## 2.4. Model development

### 2.4.1. HCN parameters

The solubility of gaseous HCN in water is governed by its Henry Law constant ( $K_{\text{H}}^0$ ):

$$(9) \quad K_{\text{H}}^0 = \frac{a_{\text{HCN}^0}}{f_{\text{HCN(g)}}} \approx \frac{a_{\text{HCN}^0}}{P_{\text{HCN(g)}}}$$

where the gas fugacity ( $f$ ) is well approximated by partial pressures ( $p$ ) at  $\sim 1$  bar. For  $K_{\text{H}}^0$  we use the temperature dependent equation from Ma et al. (2010), which investigated HCN gas solubility at low partial pressures relevant to Earth systems:

$$(10) \quad \log K_{\text{H}}^0 = -10.9978 + 3563.72 / T$$

Here and subsequently, ‘log’ is to the base 10. Once dissolved in water,  $\text{HCN}^0$  behaves as a weak acid and dissociates into  $\text{H}^+$  and  $\text{CN}^-$ . The dissociation constant for this reaction referenced to infinite dilution ( $K_{\text{HCN}}^0$ ) is given by:

$$(11) \quad K_{\text{HCN}}^0 = \frac{a_{\text{H}^+} a_{\text{CN}^-}}{a_{\text{HCN}^0}}$$

We use dissociation constants from the critical review of Kyle and Hefter (2015) (their equation 4b), and fit these values to a temperature dependent equation:

$$(12) \quad \log K_{\text{HCN}}^0 = -89.3669 + 1631.26 / T + 30.1829 \log T$$

#### 2.4.2. Ferrocyanide parameters

Aqueous cyanide strongly reacts with  $\text{Fe}^{2+}$  to form the  $\text{Fe}(\text{CN})_6^{4-}$  complex:



For the equilibrium constant in this reaction, we use  $\log K_{\text{eq}}^0 = 35.35$  at  $25^\circ\text{C}$  from Watt et al. (1965). Values at lower temperatures are not available, so we extrapolate  $K_{\text{eq}}^0$  to lower temperatures using the van't Hoff relation:

$$(14) \quad \frac{\partial \ln K_{\text{eq}}^0}{\partial T} = \frac{\Delta H_r^0}{RT^2}$$

where  $\Delta H_r^0$  is the enthalpy of reaction at  $25^\circ\text{C}$  from Watt et al. (1965) ( $-358.86 \text{ kJ mol}^{-1}$ ) and  $R$  is the molar gas constant.

We determine binary Pitzer parameters for  $\text{Na}_4\text{Fe}(\text{CN})_6$ ,  $\text{K}_4\text{Fe}(\text{CN})_6$ ,  $\text{Ca}_2\text{Fe}(\text{CN})_6$ , and  $\text{Mg}_2\text{Fe}(\text{CN})_6$  solutions over a temperature range of  $0 - 25^\circ\text{C}$  using several data sources (Fig. 1, Table 3): (1) isopiestic data at  $25^\circ\text{C}$  (this study, Table 2), (2) freezing-point depressions, and (3) osmotic pressure data at  $\sim 0^\circ\text{C}$ . Freezing point depressions give the solution water activity because the solution is in equilibrium with ice, and the equilibrium constant for ice is equal to water activity (Lewis et al., 1961), i.e.  $K_{\text{ice}}^0 = a_w$ . Osmotic pressures ( $P_{os}$ ) have been measured at  $0^\circ\text{C}$  for pure ferrocyanide salt solutions (Hartley and Burton, 1908; Hartley and Stephenson, 1909), and are related to water activities by the equation:

$$(15) \quad a_w = \exp(-P_{os} V_0 / RT)$$

where  $V_0$  is the molar volume of pure water. Experimental water activities are related osmotic coefficients via equation (4).

To fit experimental osmotic coefficient data, we assume  $\alpha_1 = 2$  and  $\alpha_2 = 1$  for the Na and K ferrocyanides, and  $\alpha_1 = 3.2$  and  $\alpha_2 = 1$  for the Ca and Mg ferrocyanides. The  $\alpha_1$  and  $\alpha_2$  parameters are used in equation (5) to calculate the  $\beta_{ca}$  parameters (see Section 2.3). We choose the values of  $\alpha_1$  and  $\alpha_2$  to accurately represent the experimental data, and as a matter of numerical convenience. We assume a temperature dependence for Pitzer parameter ( $P$ ) using the equation:

$$(16) \quad P = a_1 + a_2(T - 298.15) + a_3(T^2 - 298.15^2)$$

where  $a_i$  are fitted parameters. We do not constrain the temperature dependence of  $\text{Mg}_2\text{Fe}(\text{CN})_6$  solutions (Fig. 1D) because there is insufficient data for this salt below 25°C. Furthermore, aqueous  $\text{H}_4\text{Fe}(\text{CN})_6$  and  $\text{Fe}_2\text{Fe}(\text{CN})_6$  were not investigated in this study, so we assume their Pitzer parameterization by analogy to other salts. For  $\text{H}_4\text{Fe}(\text{CN})_6$ , we assume the  $\text{Na}_4\text{Fe}(\text{CN})_6$  parameterization, and for  $\text{Fe}_2\text{Fe}(\text{CN})_6$ , we assume the  $\text{Ca}_2\text{Fe}(\text{CN})_6$  parameterization. Overall, our Pitzer model accurately represents osmotic coefficients up to saturation (Table 3, Fig. 1); however, freezing-point depression measurements of Burrows (1923) and Fabris (1921) significantly differ from both this study and other freezing-point depression studies.

### 2.4.3. NaCN and KCN parameters

To our knowledge, water activity measurements are not available for NaCN or KCN solutions, probably because of the high toxicity of these solutions and experimental issues with the formation of HCN gas by hydrolysis. To estimate Pitzer parameters for NaCN, we use experimental  $\text{p}K_a$  values for HCN in NaCl solutions up to 5 mol  $\text{kg}^{-1}$  at 25°C (Verhoeven et al., 1990). NaCl-HCN mixtures will be governed by binary Pitzer parameters ( $\beta^{(0)}$ ,  $\beta^{(1)}$ ,  $\beta^{(2)}$ , and  $C^\phi$ ) for NaCl, NaCN, HCl, and HCN, and mixture parameters ( $\theta$  and  $\psi$ ), where the parameters involving cyanide species are unknown. Mixture parameters involving cyanide will have a minor influence on activity coefficients (Pitzer, 1991), as will binary HCN parameters, due to the relatively low concentrations of both  $\text{H}^+$  and  $\text{CN}^-$ . As a result, only the unknown binary NaCN parameters will significantly influence ion activity coefficients. Binary NaCN parameters may be estimated as follows.

The dissociation reaction  $\text{HCN}^0 = \text{H}^+ + \text{CN}^-$  is given by  $K_{\text{HCN}}$ :

$$(17) \quad K_{\text{HCN}} = \frac{[\text{H}^+][\text{CN}^-]}{[\text{HCN}^0]}$$

where square brackets indicate molal concentrations. The equilibrium constant referenced to infinite dilution ( $K_{\text{HCN}}^0$ ) for this reaction is related to  $K_{\text{HCN}}$  through the equations:

$$(18) \quad K_{\text{HCN}}^0 = \frac{a_{\text{H}^+} a_{\text{CN}^-}}{a_{\text{HCN}^0}} = \frac{\gamma_{\text{H}^+} [\text{H}^+] \gamma_{\text{CN}^-} [\text{CN}^-]}{\gamma_{\text{HCN}^0} [\text{HCN}^0]} = K_{\text{HCN}} \frac{\gamma_{\text{H}^+} \gamma_{\text{CN}^-}}{\gamma_{\text{HCN}^0}}$$

$$(19) \quad K_{\text{HCN}}^0 - K_{\text{HCN}} \frac{\gamma_{\text{H}^+} \gamma_{\text{CN}^-}}{\gamma_{\text{HCN}^0}} = 0$$

To fit experimental  $K_{\text{HCN}}$  values to our model, we apply a sum-least-squares fit to equation (19) by varying the binary NaCN Pitzer parameters (which influence the activity coefficients), where  $\text{p}K_{\text{HCN}}^0$  at 25°C is set equal to 9.21. The resulting fit accurately represents experimental  $\text{p}K_{\text{HCN}}$  values (Fig. 2, Table 3). For KCN, we assume that the Pitzer parameters are the same as for NaCN. We do not specify Pitzer parameters for  $\text{Ca}(\text{CN})_2$  and  $\text{Mg}(\text{CN})_2$  salts. As discussed in following

sections,  $\text{Ca}^{2+}$ ,  $\text{Mg}^{2+}$ , and  $\text{CN}^-$  concentrations in early Earth ferrocyanide brines are too low to significantly influence modeled activity coefficients due to carbonate precipitation.

#### 2.4.4. Solid phase equilibria

To fit solubilities in ferrocyanide solutions in our model, we use the temperature dependent equation:

$$(20) \quad \log K_{\text{eq}}^0 = a_1 + a_2 / T + a_3 T$$

where  $a_i$  are fitted parameters. With the exception of  $\text{K}_4\text{Fe}(\text{CN})_6$  solutions, solubilities in ferrocyanide solutions are poorly characterized at low temperatures, and not at all for the  $\text{Mg}_2\text{Fe}(\text{CN})_6$  system. There is some disagreement on the solubility of  $\text{Na}_4\text{Fe}(\text{CN})_6 \cdot 10\text{H}_2\text{O}$  at low temperatures, where Friend et al. (1929) predicts relatively high solubility. We choose to fit our model to the lower concentration measurements of Conroy (1898) because they are consistent with other studies at 25°C, whereas values in Friend et al. (1929) are significantly higher. For the  $\text{K}_4\text{Fe}(\text{CN})_6$ ,  $\text{Na}_4\text{Fe}(\text{CN})_6$ , and  $\text{Ca}_2\text{Fe}(\text{CN})_6$  systems, our model predicts eutectic temperatures of -1.57, -1.19, and -10.1°C respectively, which are in good agreement with literature values of -1.58 (Fabris, 1921), -1.4 (Farrow, 1927), and -10.1°C (Farrow, 1927) respectively.

We also include solubility data in mixtures containing ferrocyanide salts (Fig. 4, Fig. 5). Ferrocyanide mixtures have a marked tendency to increase the total ferrocyanide solubility relative to the single salts (Harkins and Pearce, 1916). For example, saturated  $\text{Na}_4\text{Fe}(\text{CN})_6$  and  $\text{K}_4\text{Fe}(\text{CN})_6$  solutions at 25°C contain 0.68 and 0.85 mol kg<sup>-1</sup>  $\text{Fe}(\text{CN})_6^{4-}$  respectively, whereas a Na-K- $\text{Fe}(\text{CN})_6$  mixture saturated with respect to the  $\text{Na}^+$  and  $\text{K}^+$  salts contains 2.16 mol kg<sup>-1</sup>  $\text{Fe}(\text{CN})_6^{4-}$ . The high mutual solubility of ferrocyanides is likely due to ion pairing. The Pitzer model has difficulty fitting solubilities in mixed ferrocyanides because ionic strengths in the mixtures are extremely high (22 mol kg<sup>-1</sup> in the case of Na-K- $\text{Fe}(\text{CN})_6$  mixtures), and are far beyond ionic strengths in the component binary solutions.

Experimental data on ferrocyanide solubility in chloride and carbonate mixtures is extremely limited, and we are not aware of any solubility measurements in mixtures with bicarbonate. Conroy (1898) presents solubility values for various mixtures saturated with one or more salts in carbonate and chloride solutions, but does not indicate what phases are present, so the data is of questionable use. Data is available in the Na-Cl- $\text{Fe}(\text{CN})_6$  and Na-CO<sub>3</sub>- $\text{Fe}(\text{CN})_6$  systems from Fleisher and Osokoreva (1935), and our model fits to this data are excellent (Fig. 4C, D). The general lack of data in ferrocyanide mixtures points to a need for further experimental work.

We include solubility parameters here for several sparingly soluble mixed ferrocyanides, although we note that the experimental data on these compounds is extremely limited and scattered. For sparingly soluble  $\text{CaK}_2\text{Fe}(\text{CN})_6$  and  $\text{MgK}_2\text{Fe}(\text{CN})_6$  salts, we estimate the solubility temperature dependence by assuming a linear trend from ~20 to 100°C (Fig. 5). A  $\text{Fe}_2[\text{Fe}(\text{CN})_6]$  salt, Berlin White, is also known to form, which is related to the compound Prussian Blue (Williams, 1915). We are aware of only one literature value of 1.4 x 10<sup>-5</sup> mol kg<sup>-1</sup> at pH 6 for the solubility of this salt (Hendrickson and Daignault, 1973). This solubility is similar to other salts of the type  $\text{M}_2\text{Fe}(\text{CN})_6$ , where M is a transition metal cation (Tananaev et al., 1956).

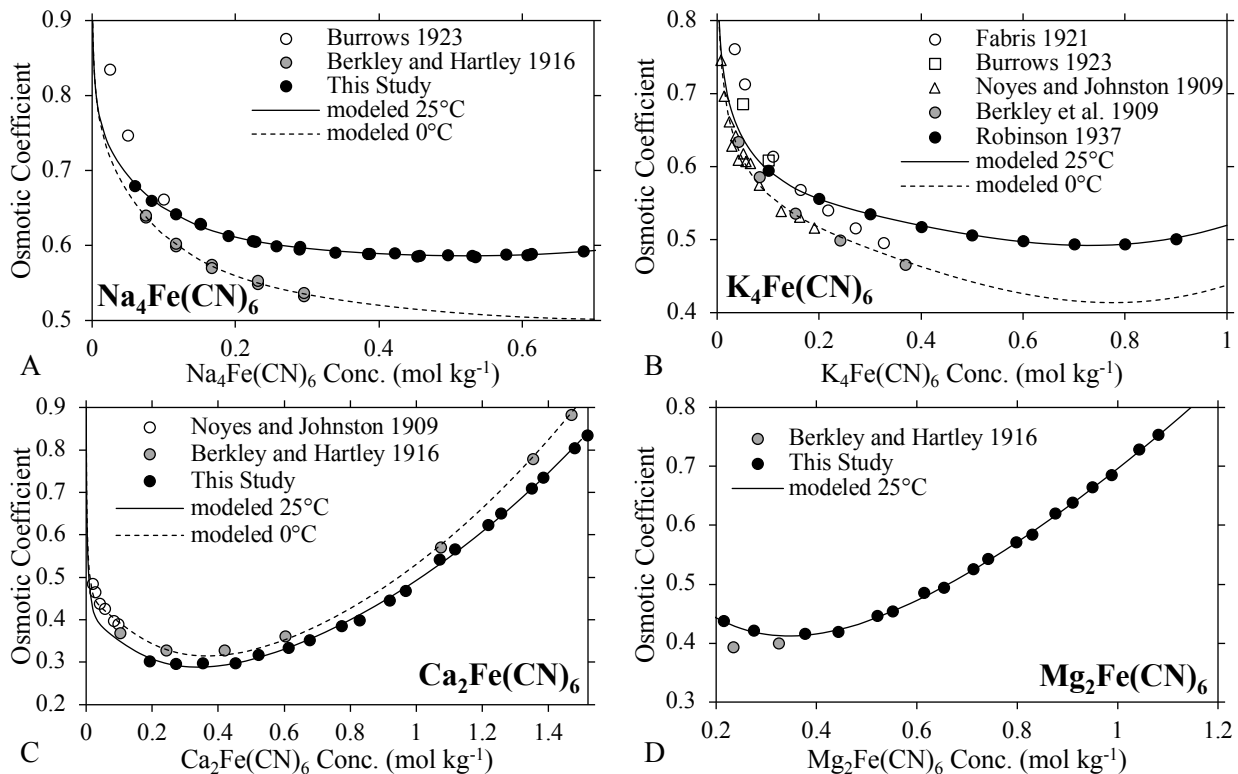


Fig. 1. Osmotic coefficients in (A) Na<sub>4</sub>Fe(CN)<sub>6</sub>, (B) K<sub>4</sub>Fe(CN)<sub>6</sub>, (C) Ca<sub>2</sub>Fe(CN)<sub>6</sub>, and (D) Mg<sub>2</sub>Fe(CN)<sub>6</sub> solutions from isopiestic measurements from this study and others (Robinson, 1937) (black circles), osmotic pressure measurements (Hartley and Burton, 1908; Hartley and Stephenson, 1909) (gray circles), and freezing-point depression measurements (Burrows, 1923; Fabris, 1921; Noyes and Johnston, 1909) (hollow symbols).

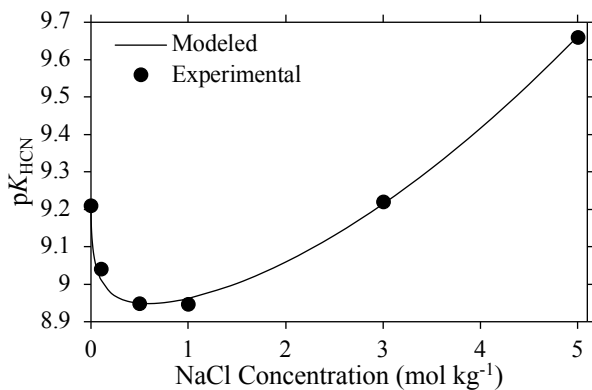


Fig. 2. Experimental pK<sub>a</sub> values for HCN<sup>0</sup> in NaCl solutions from Verhoeven et al. (1990). (circles), and modeled pK<sub>a</sub> values (solid line).

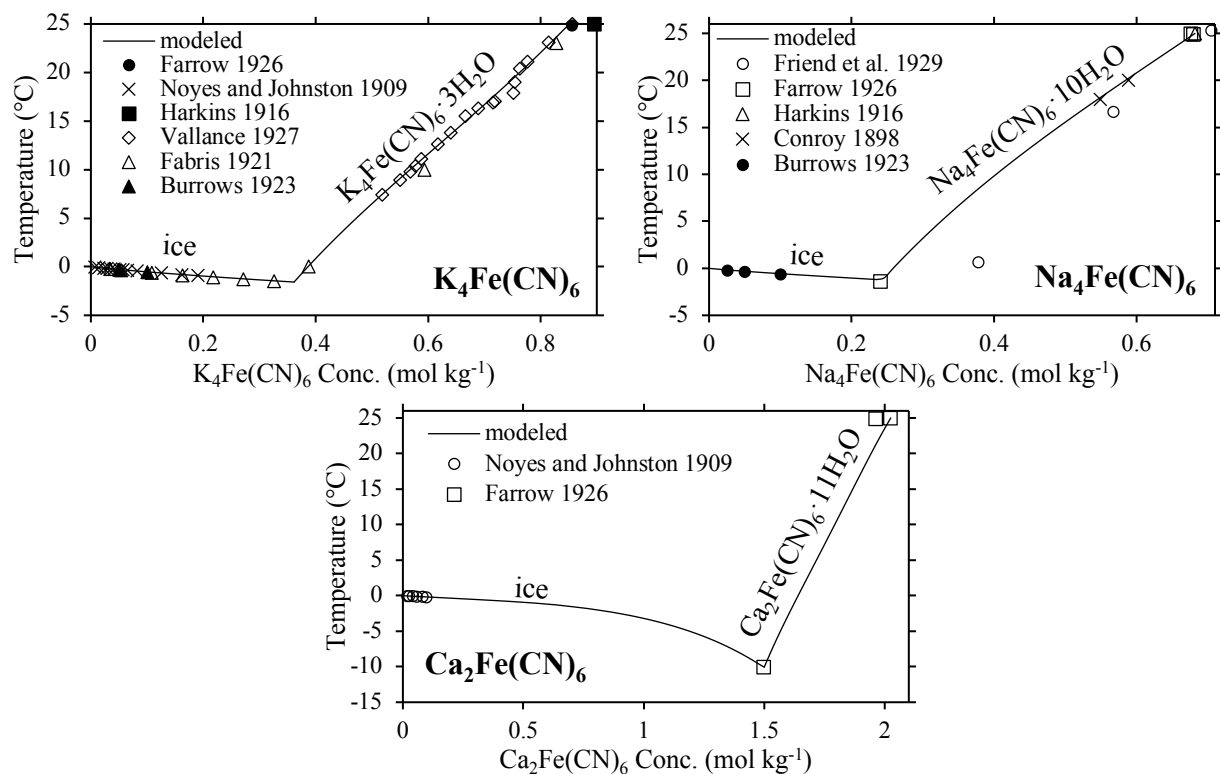


Fig. 3. Experimental data (symbols) (Burrows, 1923; Conroy, 1898; Fabris, 1921; Farrow, 1926, 1927; Friend et al., 1929; Harkins and Pearce, 1916; Noyes and Johnston, 1909; Vallance, 1927) and modeled curves (black lines) in  $K_4Fe(CN)_6$ ,  $Na_4Fe(CN)_6$ , and  $Ca_2Fe(CN)_6$  solutions.

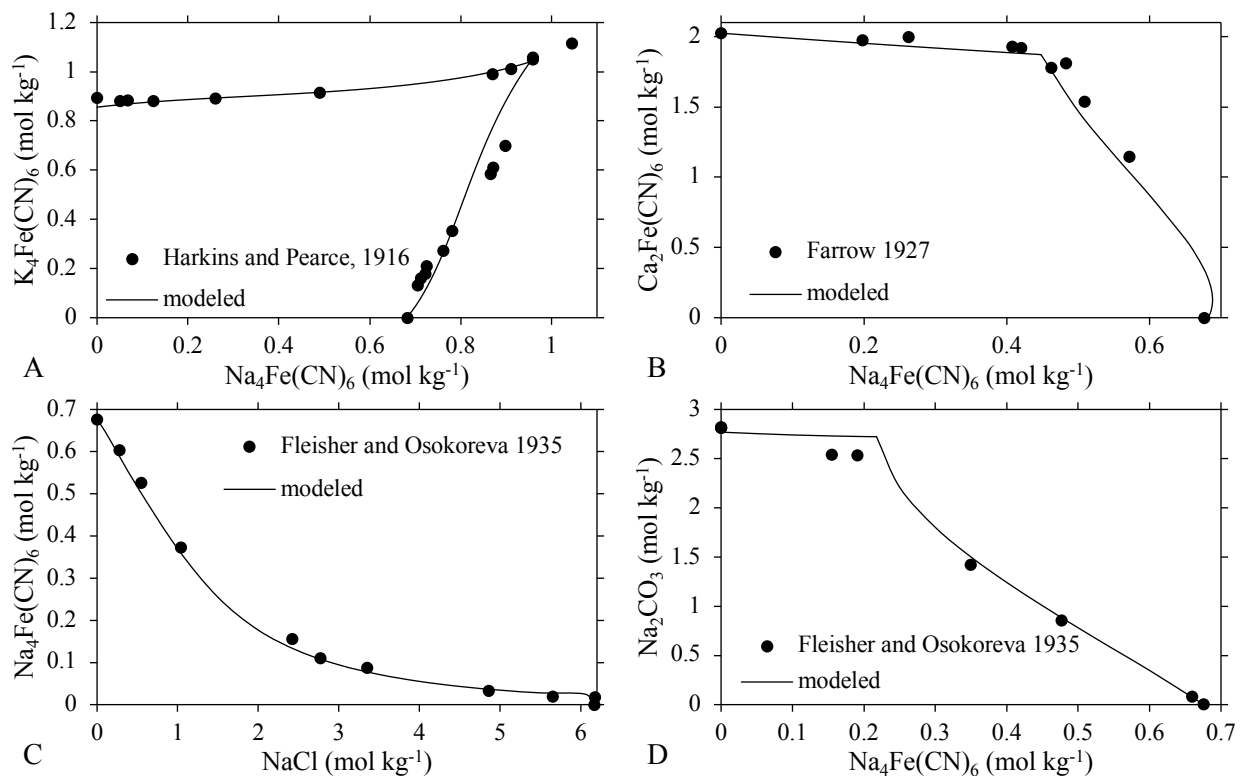


Fig. 4. Experimental solubilities (symbols) in Na-K-Fe(CN)<sub>6</sub> (A) (Harkins and Pearce, 1916), Na-Ca-Fe(CN)<sub>6</sub> (B) (Farrow, 1927), Na-Cl-Fe(CN)<sub>6</sub> (C) (Fleisher and Osokoreva, 1935), and Na-CO<sub>3</sub>-Fe(CN)<sub>6</sub> (D) (Fleisher and Osokoreva, 1935) systems. Solid lines are modeled values.

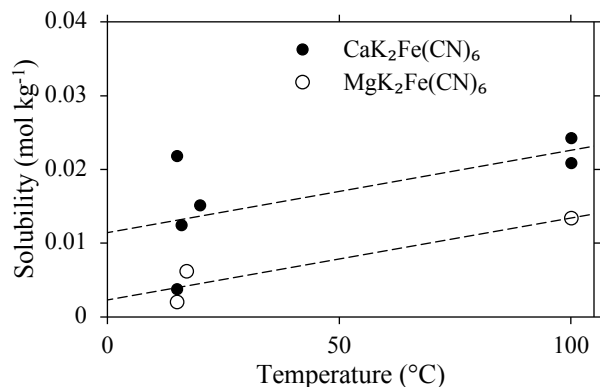


Fig. 5. The solubility of  $\text{CaK}_2\text{Fe}(\text{CN})_6$  and  $\text{MgK}_2\text{Fe}(\text{CN})_6$  salts as a function of temperature from various data sources (Brown, 1907; Comey and Hahn, 1921; de Rada and Bermejo, 1929; Robinson, 1909; Williams, 1915). Dashed lines are linear fits used to estimate the solubility temperature dependence.

Table 1. Concentrations of stock solutions used in the isopiestic experiments.

Salt	Stock Concentration (mol·kg <sup>-1</sup> )
NaCl	6.078 ± 0.002
Na <sub>4</sub> Fe(CN) <sub>6</sub>	0.524 ± 0.001
Ca <sub>2</sub> Fe(CN) <sub>6</sub>	1.560 ± 0.010
Mg <sub>2</sub> Fe(CN) <sub>6</sub>	1.187 ± 0.002

Table 2. Osmotic coefficients ( $\phi$ ) derived from isopiestic experiments using NaCl as the reference solution and Na<sub>4</sub>Fe(CN)<sub>6</sub>, Mg<sub>2</sub>Fe(CN)<sub>6</sub>, and Ca<sub>2</sub>Fe(CN)<sub>6</sub> as the sample solutions. Here the  $m$  is the molal concentration (mol kg<sup>-1</sup>).

$m_{\text{NaCl}}$	$m_{\text{Na}_4\text{Fe}(\text{CN})_6}$	$\phi$	$m_{\text{NaCl}}$	$m_{\text{Mg}_2\text{Fe}(\text{CN})_6}$	$\phi$	$m_{\text{NaCl}}$	$m_{\text{Ca}_2\text{Fe}(\text{CN})_6}$	$\phi$
0.1092	0.0598	0.6800	0.1517	0.2143	0.4372	0.0933	0.1921	0.3022
0.1478	0.0830	0.6602	0.1881	0.2750	0.4213	0.1304	0.2721	0.2966
0.2031	0.1169	0.6419	0.2550	0.3772	0.4154	0.1706	0.3535	0.2977
0.2575	0.1509	0.6290	0.3022	0.4431	0.4187	0.2191	0.4519	0.2982
0.2587	0.1517	0.6286	0.3786	0.5213	0.4458	0.2686	0.5210	0.3167
0.3163	0.1900	0.6131	0.4086	0.5520	0.4544	0.3328	0.6125	0.3335
0.3688	0.2239	0.6066	0.4852	0.6143	0.4853	0.3876	0.6765	0.3517
0.3744	0.2277	0.6055	0.5252	0.6533	0.4942	0.4837	0.7732	0.3844
0.4176	0.2566	0.5994	0.6082	0.7123	0.5261	0.5371	0.8274	0.3992
0.4663	0.2888	0.5950	0.6530	0.7418	0.5431	0.6631	0.9179	0.4459
0.4701	0.2896	0.5982	0.7362	0.7981	0.5706	0.7305	0.9667	0.4674
0.5433	0.3392	0.5911	0.7827	0.8298	0.5844	0.9299	1.0703	0.5413
0.6129	0.3844	0.5895	0.8725	0.8751	0.6199	1.0112	1.1158	0.5666
0.6172	0.3874	0.5890	0.9320	0.9094	0.6386	1.2018	1.2172	0.6226
0.6720	0.4220	0.5898	1.0096	0.9494	0.6648	1.2890	1.2563	0.6497
0.7166	0.4535	0.5860	1.0793	0.9873	0.6854	1.4957	1.3490	0.7094
0.7212	0.4563	0.5864	1.2040	1.0428	0.7281	1.5815	1.3839	0.7346
0.7847	0.4963	0.5878	1.2855	1.0803	0.7534	1.8259	1.4793	0.8041
0.8335	0.5295	0.5863	-	-	-	1.9312	1.5178	0.8339
0.8391	0.5348	0.5845	-	-	-	-	-	-
0.9083	0.5770	0.5880	-	-	-	-	-	-
0.9525	0.6063	0.5878	-	-	-	-	-	-
0.9598	0.6109	0.5881	-	-	-	-	-	-
0.9639	0.6128	0.5888	-	-	-	-	-	-
1.0789	0.6853	0.5922	-	-	-	-	-	-

Table 3. Values for temperature dependent binary Pitzer parameters used in equation (16).

parameter	$a_0$	$a_1$	$a_2$
$\beta_{\text{Na}_4\text{Fe}(\text{CN})_6}^{(0)}$ <sup>a</sup>	5.1895E-01	-7.1016E-03	–
$\beta_{\text{Na}_4\text{Fe}(\text{CN})_6}^{(1)}$ <sup>a</sup>	9.5653E+00	-5.3788E-02	–
$\beta_{\text{Na}_4\text{Fe}(\text{CN})_6}^{(2)}$ <sup>a</sup>	1.3045E+00	7.8866E-02	–
$C_{\text{Na}_4\text{Fe}(\text{CN})_6}^\phi$ <sup>a</sup>	-9.6713E-02	3.7854E-03	–
$\beta_{\text{K}_4\text{Fe}(\text{CN})_6}^{(0)}$	3.9931E-01	7.6200E-03	–
$\beta_{\text{K}_4\text{Fe}(\text{CN})_6}^{(1)}$	7.1211E+00	7.7346E-02	–
$\beta_{\text{K}_4\text{Fe}(\text{CN})_6}^{(2)}$	1.5967E+00	-1.0196E-02	–
$C_{\text{K}_4\text{Fe}(\text{CN})_6}^\phi$	-7.7655E-02	-2.6467E-03	–
$\beta_{\text{Ca}_2\text{Fe}(\text{CN})_6}^{(0)}$ <sup>b</sup>	7.6812E-01	-4.7633E-01	8.4030E-04
$\beta_{\text{Ca}_2\text{Fe}(\text{CN})_6}^{(1)}$ <sup>b</sup>	4.5582E+01	4.1868E+01	-7.2742E-02
$\beta_{\text{Ca}_2\text{Fe}(\text{CN})_6}^{(2)}$ <sup>b</sup>	1.2530E+01	–	–
$C_{\text{Ca}_2\text{Fe}(\text{CN})_6}^\phi$ <sup>b</sup>	2.5717E-02	-7.4208E-03	-2.1868E-04
$\beta_{\text{Mg}_2\text{Fe}(\text{CN})_6}^{(0)}$	8.0940E-01	–	–
$\beta_{\text{Mg}_2\text{Fe}(\text{CN})_6}^{(1)}$	6.4514E+01	–	–
$\beta_{\text{Mg}_2\text{Fe}(\text{CN})_6}^{(2)}$	1.3903E+01	–	–
$C_{\text{Mg}_2\text{Fe}(\text{CN})_6}^\phi$	7.5225E-02	–	–
$\beta_{\text{NaCN}}^{(0)}$ <sup>c</sup>	-1.0350E-01	–	–
$\beta_{\text{NaCN}}^{(1)}$ <sup>c</sup>	7.3860E-01	–	–
$C_{\text{NaCN}}^\phi$ <sup>c</sup>	4.0660E-02	–	–

<sup>a</sup>Parameters also assumed for  $\text{H}_4\text{Fe}(\text{CN})_6$ .

<sup>b</sup>Parameters also assumed for  $\text{Fe}_2\text{Fe}(\text{CN})_6$ .

<sup>c</sup>Parameters also assumed for KCN.

Table 4. Values for Pitzer mixing parameters.

$\theta_{\text{Cl}^-, \text{Fe}(\text{CN})_6^{4-}}$ <sup>a</sup>	4.6084E-01
$\theta_{\text{CO}_3^{2-}, \text{Fe}(\text{CN})_6^{4-}}$	4.7093E-01
$\psi_{\text{Na}^+, \text{K}^+, \text{Fe}(\text{CN})_6^{4-}}$	4.7936E-02
$\psi_{\text{Na}^+, \text{Ca}^{2+}, \text{Fe}(\text{CN})_6^{4-}}$	2.1145E-02
$\psi_{\text{CO}_3^{2-}, \text{Fe}(\text{CN})_6^{4-}, \text{Na}^+}$ <sup>b</sup>	-4.0723E-02
$\psi_{\text{Cl}^-, \text{Fe}(\text{CN})_6^{4-}, \text{Na}^+}$ <sup>c</sup>	-3.1177E-03

<sup>a</sup>Parameter also assumed for  $\theta_{\text{HCO}_3^-, \text{Fe}(\text{CN})_6^{4-}}$ .

<sup>b</sup>Parameter also assumed for  $\psi_{\text{CO}_3^{2-}, \text{Fe}(\text{CN})_6^{4-}, \text{K}^+}$ .

<sup>c</sup>Parameter also assumed for  $\psi_{\text{HCO}_3^-, \text{Fe}(\text{CN})_6^{4-}, \text{Na}^+}$ ,  $\psi_{\text{HCO}_3^-, \text{Fe}(\text{CN})_6^{4-}, \text{K}^+}$ , and  $\psi_{\text{Cl}^-, \text{Fe}(\text{CN})_6^{4-}, \text{K}^+}$ .

Table 5. Solubility parameters for  $\log K^0$  used in equation (20).

Salt	$a_0$	$a_1$	$a_2$
$\text{Na}_4\text{Fe}(\text{CN})_6 \cdot 10\text{H}_2\text{O}$	10.723	-4437.72	–
$\text{K}_4\text{Fe}(\text{CN})_6 \cdot 3\text{H}_2\text{O}$	7.311	-3531	–
$\text{Ca}_2\text{Fe}(\text{CN})_6 \cdot 11\text{H}_2\text{O}$	-7.481	–	0.010516
$\text{CaK}_2\text{Fe}(\text{CN})_6$	-2.163	-431.70	-0.00144
$\text{MgK}_2\text{Fe}(\text{CN})_6$	36.883	-6633.77	-0.06389
$\text{Fe}_2[\text{Fe}(\text{CN})_6]$	-14.115	–	–

### 3. Appendix C: Supplement to frezchem.dat in PHREEQC

The following PHREEQC input code may be used in conjunction with the frezchem.dat database. For example, this code may be pasted into the interactive version of PHREEQC (available at [https://wwwbr.c.usgs.gov/projects/GWC\\_coupled/phreeqc/](https://wwwbr.c.usgs.gov/projects/GWC_coupled/phreeqc/)). Note that the frezchem.dat database needs to be selected independently from entering the input code below. If using the interactive version of PHREEQC, the definitions of all input parameters given below are well-described in the program. We have commented on the code primarily to specify the source reference for specific parameters.

```
#The iron parameters in this supplementary phreeqc file are from:
#Marion, G. M., et al. (2003). Modeling aqueous ferrous iron chemistry at
#low temperatures with application to Mars.
#Geochimica et Cosmochimica Acta 67(22): 4251-4266.
#
#The HCN Henry Law Constant is from:
#Ma, J., et al. (2010). Temperature dependence of Henry's law constant
#for hydrogen cyanide. Generation of trace standard gaseous hydrogen cyanide.
#Environmental Science & Technology 44(8): 3028-3034.
#
#The ferrocyanide dissociation constant is from:
#Watt, G. D., et al. (1965). Thermodynamics of Metal Cyanide Coordination.
#III.  $\Delta G^\circ$ ,  $\Delta H^\circ$ , and  $\Delta S^\circ$  Values for Ferrocyanide and Ferricyanide Ion
#Formation in Aqueous Solution at 25°." Inorganic Chemistry 4(2): 220-222.
#
#The HCN dissociation constant is from:
# Kyle, J. H. and G. Hefter (2015). A critical review of the thermodynamics
#of hydrogen cyanide and copper (I)-cyanide complexes in aqueous solution.
#Hydrometallurgy 154: 78-87.

#This establishes Fe2+ and CN- as elements.
SOLUTION_MASTER_SPECIES
  Fe Fe+2 0 Fe 55.847
  Cn Cn- 1 26.02 26.02

#This defines aqueous species and speciation reactions.
SOLUTION_SPECIES
Fe+2 = Fe+2
  log_k 0
Cn- = Cn-
  log_k 0
Fe+2 + H2O = FeOH+ + H+ #Marion et al. 2003
  -analytical_expression 0.170687263 0 -2883.370079 0 0 0
CO3-2 + Fe+2 = FeCO3 #Marion et al. 2003
  -analytical_expression 6.368491354 0 -592.8753207 0 0 0
6Cn- + Fe+2 = Fe(Cn)6-4 #Watt et al. 1965
  log_k 35.35284705
  delta_h -358.86168 kJ
Cn- + H+ = HCN #Kyle and Hefter 2015
  -analytical_expression 89.3669 0 -1631.26 -30.1829 0 0

#This defines solid and gas-phase reactions.
```

PHASES

FeCl2:4H2O #Marion et al. 2003  
 $\text{FeCl}_2:4\text{H}_2\text{O} = 2\text{Cl}^- + \text{Fe}^{+2} + 4\text{H}_2\text{O}$   
 -analytical\_expression -1.995530577 0.063290169 0 0 0 -0.000150325

FeCl2:6H2O #Marion et al. 2003  
 $\text{FeCl}_2:6\text{H}_2\text{O} = 2\text{Cl}^- + \text{Fe}^{+2} + 6\text{H}_2\text{O}$   
 -analytical\_expression -2666.89 -5.333 -0.11245 1532.3717 -0.000856 0.005274

FeSO4:H2O #Marion et al. 2003  
 $\text{FeSO}_4:\text{H}_2\text{O} = \text{Fe}^{+2} + \text{H}_2\text{O} + \text{SO}_4^{-2}$   
 -analytical\_expression 2.746622489 -0.01212333 0 0 0 0

FeSO4:7H2O #Marion et al. 2003  
 $\text{FeSO}_4:7\text{H}_2\text{O} = \text{Fe}^{+2} + 7\text{H}_2\text{O} + \text{SO}_4^{-2}$   
 -analytical\_expression 9.10362447 -0.101770354 0 0 0 0.000214023

Siderite #Marion et al. 2003  
 $\text{FeCO}_3 = \text{CO}_3^{-2} + \text{Fe}^{+2}$   
 -analytical\_expression -12.87856857 0 542.1949459 0 0 0

K4Fe(CN)6:3H3O #This study  
 $\text{K}_4\text{Fe}(\text{Cn})_6:3\text{H}_2\text{O} = \text{Fe}(\text{Cn})_6^{-4} + 3\text{H}_2\text{O} + 4\text{K}^+$   
 log\_k -4.53180813  
 -analytical\_expression 7.3112 0 -3530.993956 0 0 0

Na4Fe(CN)6:10H2O #This study  
 $\text{Na}_4\text{Fe}(\text{Cn})_6:10\text{H}_2\text{O} = \text{Fe}(\text{Cn})_6^{-4} + 10\text{H}_2\text{O} + 4\text{Na}^+$   
 log\_k -4.160962139  
 -analytical\_expression 10.7232 0 -4437.719719 0 0 0

Ca2Fe(CN)6:11H2O #This study  
 $\text{Ca}_2\text{Fe}(\text{Cn})_6:11\text{H}_2\text{O} = 2\text{Ca}^{+2} + \text{Fe}(\text{Cn})_6^{-4} + 11\text{H}_2\text{O}$   
 log\_k -4.345811225  
 -analytical\_expression -7.4812 0.010516124 0 0 0 0

CaK2Fe(CN)6 #This study  
 $\text{CaK}_2\text{Fe}(\text{Cn})_6 = \text{Ca}^{+2} + \text{Fe}(\text{Cn})_6^{-4} + 2\text{K}^+$   
 log\_k -4.040936436  
 -analytical\_expression -6.70193 0.0144557 0 0 0 -1.85506e-05

MgK2Fe(CN)6 #This study  
 $\text{MgK}_2\text{Fe}(\text{Cn})_6 = \text{Fe}(\text{Cn})_6^{-4} + 2\text{K}^+ + \text{Mg}^{+2}$   
 log\_k -4.416470875  
 -analytical\_expression -32.8085 0.180024 0 0 0 -0.000284432

Fe2Fe(CN)6 #This study  
 $\text{Fe}_2\text{Fe}(\text{Cn})_6 = \text{Fe}(\text{Cn})_6^{-4} + 2\text{Fe}^{+2}$   
 log\_k -14.115

HCN(g) #Ma et al. 2010  
 $\text{HCn} = \text{HCn}$   
 -analytical\_expression -10.9978 0 3563.72 0 0 0

#This defines the temperature dependence of Pitzer parameters

PITZER

-MacInnes false  
 -use\_etheta true  
 -redox false  
 -B0

#The following are from Marion et al. 2003

Fe+2 Cl- 0.3359  
 Fe+2 HCO3- -0.009295803 -273406.17 -2607.1152 8.250840001 -0.00434  
 Fe+2 SO4-2 0.256867423 -1389.639805 0 -0.038599989 3.91e-05

```

FeOH+ Cl- -0.1
#The following are from this study
K+ Fe(Cn)6-4 0.399306384 0 0 0.007619972
Na+ Fe(Cn)6-4 0.518949868 0 0 -0.007101609
H+ Fe(Cn)6-4 0.518949868 0 0 -0.007101609
Mg+2 Fe(Cn)6-4 0.80939897
Ca+2 Fe(Cn)6-4 0.76812043 0 0 -0.476327898 0.000840304
Fe+2 Fe(Cn)6-4 0.76812043 0 0 -0.476327898 0.000840304
Na+ Cn- -0.107171
K+ Cn- -0.107171
-B1
#The following are from Marion et al. 2003
Fe+2 Cl- 1.53226 0 0 -0.1236
Fe+2 HCO3- 0.80280979 3203209.7 29927.152 -92.77793501 0.0477642
Fe+2 SO4-2 3.08794218 0 0 -0.6383194 0.001190408
FeOH+ Cl- 1.658
#The following are from this study
K+ Fe(Cn)6-4 7.121131114 0 0 0.07734604
Na+ Fe(Cn)6-4 9.565313466 0 0 -0.053787617
H+ Fe(Cn)6-4 9.565313466 0 0 -0.053787617
Mg+2 Fe(Cn)6-4 64.51407273
Ca+2 Fe(Cn)6-4 45.58242694 0 0 41.86781959 -0.072742214
Fe+2 Fe(Cn)6-4 45.58242694 0 0 41.86781959 -0.072742214
Na+ Cn- 0.737849
K+ Cn- 0.737849
-B2
#The following are from Marion et al. 2003
Fe+2 SO4-2 -42
#The following are from this study
K+ Fe(Cn)6-4 1.596664742 0 0 -0.010195586
Na+ Fe(Cn)6-4 1.304547634 0 0 0.07886574
H+ Fe(Cn)6-4 1.304547634 0 0 0.07886574
Mg+2 Fe(Cn)6-4 13.90341246
Ca+2 Fe(Cn)6-4 12.529785
Fe+2 Fe(Cn)6-4 12.529785
-C0
#The following are from Marion et al. 2003
Fe+2 Cl- -0.00861
Fe+2 HCO3- 0
Fe+2 SO4-2 0.0209
#The following are from this study
K+ Fe(Cn)6-4 -0.077655357 0 0 -0.00264668
Na+ Fe(Cn)6-4 -0.096712652 0 0 0.003785379
H+ Fe(Cn)6-4 -0.096712652 0 0 0.003785379
Mg+2 Fe(Cn)6-4 0.075224792
Ca+2 Fe(Cn)6-4 0.025716506 0 0 -0.007420783 -0.000218676
Fe+2 Fe(Cn)6-4 0.025716506 0 0 -0.007420783 -0.000218676
Na+ Cn- 0.041681
K+ Cn- 0.041681
-PSI
#The following are from Marion et al. 2003
Na+ Fe+2 Cl- -0.014
Na+ Fe+2 SO4-2 -0.0098 -0.00308 0.22885 -0.000294 -2.48404e-07 -6.49474e-05

```

K+ Fe+2 Cl- -0.049482781 -28.99088741 0 -8.75059e-06  
K+ Fe+2 SO4-2 -0.124386 0.0066217 -0.4917308 0.0023847 -2.7475e-06 0.0001049  
H+ Fe+2 Cl- 0.01197725 0 0 0.000515  
Ca+2 Fe+2 Cl- -0.023810091 -981.6585215 -7.406198558 0.013037731  
Ca+2 Fe+2 SO4-2 0.024  
Cl- SO4-2 Fe+2 -0.0183068 -0.032188 0.3308 -0.0015546 1.15824e-06 -0.0011574  
Cl- HCO3- Fe+2 -0.096  
SO4-2 HCO3- Fe+2 -0.161  
Fe+2 FeOH+ Cl- 0.028  
#The following are from this study  
Na+ K+ Fe(Cn)6-4 0.047935547  
Na+ Ca+2 Fe(Cn)6-4 0.021145366  
Fe(Cn)6-4 CO3-2 Na+ -0.040718389  
Fe(Cn)6-4 CO3-2 K+ -0.040718389  
Fe(Cn)6-4 Cl- Na+ -0.003117718  
Fe(Cn)6-4 Cl- K+ -0.003117718  
Fe(Cn)6-4 HCO3 Na+ -0.003117718  
Fe(Cn)6-4 HCO3- K+ -0.003117718  
-THETA  
#The following are from Marion et al. 2003  
Na+ Fe+2 0.08  
K+ Fe+2 0.1167  
Ca+2 Fe+2 0.124367406 -983.1138482 0 -0.006342425  
#The following are from this study  
Cl- Fe(Cn)6-4 0.460841574  
HCO3- Fe(Cn)6-4 0.460841574  
CO3-2 Fe(Cn)6-4 0.470926735  
-LAMDA  
#The following are from Marion et al. 2003  
Fe+2 CO2 0.1447325 3589.5040984 104.345457 -0.5418434 0.0003881 -0.916659  
-ETA  
#The following are from Marion et al. 2003  
CO2 Fe+2 Cl- -0.009846951 27726.80974 253.623194 -0.772286 0.000391603  
CO2 Fe+2 SO4-2 -0.041586353 143162.6076 1412.302898 -4.608331 0.002489207  
-ALPHAS  
#The following are from this study  
K+ Fe(Cn)6-4 2 1  
Na+ Fe(Cn)6-4 2 1  
H+ Fe(Cn)6-4 2 1  
Ca+2 Fe(Cn)6-4 3.2 1  
Mg+2 Fe(Cn)6-4 3.2 1  
Fe+2 Fe(Cn)6-4 3.2 1

## Supplementary References

- Brown, J.C. (1907) Some double ferrocyanides of calcium, potassium, and ammonium. *Journal of the Chemical Society, Transactions* 91, 1826-1831.
- Burrows, G.J. (1923) Dissociation of complex cyanides. *Journal of the Chemical Society, Transactions* 123, 2026-2029.
- Cleaves II, H.J. (2008) The prebiotic geochemistry of formaldehyde. *Precambrian Res.* 164, 111-118.
- Comey, A.M. and Hahn, D.A. (1921) *A Dictionary of Chemical Solubilities: Inorganic*, 2nd ed. The Macmillan Company, New York.
- Conroy, J.T. (1898) Composition and solubility of sodium ferrocyanide. *Journal of the Society of Chemical Industry* 17, 103-106.
- de Rada, F.D. and Bermejo, A.G. (1929) Determination of the solubilities of various ferrocyanides in alcohol-water mixtures. *Anales de la Real Sociedad Española de Física y Química* 27, 701-711.
- Fabris, E. (1921) Solubility of potassium ferrocyanide in water. The ice curve and cryohydric point. *Gazz. Chim. Ital.* 51, 374-380.
- Farrow, M. (1926) The solubilities of sodium, potassium, and calcium ferrocyanides. Part I. *Journal of the Chemical Society (Resumed)* 129, 49-55.
- Farrow, M. (1927) The system calcium ferrocyanide–sodium ferrocyanide–water. Part II. *Journal of the Chemical Society (Resumed)*, 1153-1158.
- Fegley Jr, B., Prinn, R.G., Hartman, H. and Watkins, G.H. (1986) Chemical effects of large impacts on the Earth's primitive atmosphere. *Nature* 319, 305-308.
- Fleisher, N.A. and Osokoreva, N.A. (1935) Salt equilibria in aqueous solutions of sodium ferrocyanide, sodium chloride, sodium carbonate and sodium sulfate at 25°. *Gosudarstvennyj Institut Prikladnoj Chimii* 26, 23-38.
- Friend, J.A.N., Townley, J.E. and Vallance, R.H. (1929) The solubility of sodium ferrocyanide in water between 0° and 104°. *Journal of the Chemical Society (Resumed)*, 2326-2330.
- Harkins, W.D. and Pearce, W.T. (1916) The effect of salts upon the solubility of other salts. VII. The solubility relations of some extremely soluble salts. *J. Am. Chem. Soc.* 38, 2714-2717.
- Hartley, E.G.J. and Burton, C.V. (1908) On the osmotic pressures of aqueous solutions of calcium ferrocyanide. Part. I—Concentrated solutions. *Philosophical Transactions of the Royal Society of London. Series A* 81, 177-203.
- Hartley, E.G.J. and Stephenson, J. (1909) Osmotic Pressures of Calcium Ferrocyanide Solutions. Part II: Weak Solutions. *Philosophical Transactions of the Royal Society of London. Series A* 209, 319-336.
- Harvie, C.E. and Weare, J.H. (1980) The prediction of mineral solubilities in natural waters: the Na-K-Mg-Ca-Cl-SO<sub>4</sub>-H<sub>2</sub>O system from zero to high concentration at 25° C. *Geochim. Cosmochim. Acta* 44, 981-997.
- Hendrickson, T.N. and Daignault, L.G. (1973) Treatment of photographic ferrocyanide-type bleach solutions for reuse and disposal. *Journal of the SMPTE* 82, 727-732.
- Kyle, J.H. and Hefter, G. (2015) A critical review of the thermodynamics of hydrogen cyanide and copper (I)–cyanide complexes in aqueous solution. *Hydrometallurgy* 154, 78-87.
- Lewis, G.N., Randall, M., Pitzer, K.S. and Brewer, L. (1961) *Thermodynamics*, second ed. McGraw-Hill.
- Luthy, R.G. and Bruce Jr, S.G. (1979) Kinetics of reaction of cyanide and reduced sulfur species in aqueous solution. *Environ. Sci. Technol.* 13, 1481-1487.

- Ma, J., Dasgupta, P.K., Blackledge, W. and Boss, G.R. (2010) Temperature dependence of Henry's law constant for hydrogen cyanide. Generation of trace standard gaseous hydrogen cyanide. *Environ. Sci. Technol.* 44, 3028-3034.
- Marion, G.M. and Kargel, J.S. (2008) Cold aqueous planetary geochemistry with FREZCHEM: From modeling to the search for life at the limits. Springer, Berlin/Heidelberg.
- Miyakawa, S., Cleaves, H.J. and Miller, S.L. (2002) The cold origin of life: A. Implications based on the hydrolytic stabilities of hydrogen cyanide and formamide. *Origins Life Evol. Biosphere* 32, 195-208.
- Noyes, A.A. and Johnston, J. (1909) The conductivity and ionization of polyionic salts. *J. Am. Chem. Soc.* 31, 987-1010.
- Parkos, D., Pikus, A., Alexeenko, A. and Melosh, H.J. (2018) HCN production via impact ejecta reentry during the Late Heavy Bombardment. *Journal of Geophysical Research: Planets* 123, 892-909.
- Pitzer, K.S. (1991) Ion interaction approach: Theory and data correlation, *Activity Coefficients in Electrolyte Solutions*, second ed. CRC Press, Boca Raton, pp. 75-153.
- Pitzer, K.S. and Mayorga, G. (1974) Thermodynamics of electrolytes. III. Activity and osmotic coefficients for 2-2 electrolytes. *J. Solution Chem.* 3, 539-546.
- Platford, R.F. (1979) Experimental Methods: Isopiestic, in: Pytkowicz, R.M. (Ed.), *Activity Coefficients in Electrolyte Solutions*. CRC Press, Inc., Boca Raton, FL.
- Robinson, F.W. (1909) Double and triple ferrocyanides of magnesium, aluminium, and cerium with potassium and ammonium. *Journal of the Chemical Society, Transactions* 95, 1353-1359.
- Robinson, R.A. (1937) The osmotic and activity coefficient data of some aqueous salt solutions from vapor pressure measurements. *J. Am. Chem. Soc.* 59, 84-90.
- Schlesinger, G. and Miller, S.L. (1973) Equilibrium and kinetics of glyconitrile formation in aqueous solution. *J. Am. Chem. Soc.* 95, 3729-3735.
- Tananaev, I.V., Glushkova, M.A. and Seifer, G.B. (1956) The solubility series of ferrocyanides. *Journal of Inorganic Chemistry - USSR* 1, 72-74.
- Toner, J.D. and Catling, D.C. (2018) Chlorate brines on Mars: Implications for the occurrence of liquid water and deliquescence. *Earth. Planet. Sci. Lett.* 497, 161-168.
- Vallance, R.H. (1927) The solubility of potassium ferrocyanide in water at temperatures up to 25°. *Journal of the Chemical Society (Resumed)*, 1328-1334.
- Verhoeven, P., Hefter, G. and May, P.M. (1990) Dissociation constant of hydrogen cyanide in saline solutions. *Miner. Metall. Process* 7, 185-188.
- Watt, G.D., Christensen, J.J. and Izatt, R.M. (1965) Thermodynamics of Metal Cyanide Coordination. III.  $\Delta G^\circ$ ,  $\Delta H^\circ$ , and  $\Delta S^\circ$  Values for Ferrocyanide and Ferricyanide Ion Formation in Aqueous Solution at 25°. *Inorg. Chem.* 4, 220-222.
- Williams, H.E. (1915) *The chemistry of cyanogen compounds and their manufacture and estimation*. J. & A. Churchill, London.
- Zahnle, K., Claire, M. and Catling, D. (2006) The loss of mass-independent fractionation in sulfur due to a Palaeoproterozoic collapse of atmospheric methane. *Geobiology* 4, 271-283.
- Zahnle, K.J. (1986) Photochemistry of methane and the formation of hydrocyanic acid (HCN) in the Earth's early atmosphere. *Journal of Geophysical Research: Atmospheres* 91, 2819-2834.